Negative feedback between the APC/C and Cep152 at the centrosome regulates mitotic spindle assembly

Thomas Tischer[1,*], Jing Yang[1] and David Barford[1]

[1] MRC Laboratory of Molecular Biology, Francis Crick Avenue, Cambridge, CB2 0QH, UK

[*] corresponding author: ttischer@mrc-lmb.cam.ac.uk

Abstract

The control of protein abundance is a fundamental regulatory mechanism during mitosis. The anaphase promoting complex/cyclosome (APC/C) is the main protein ubiquitin ligase responsible for regulating mitotic progression in a timely manner. Previous studies proposed that the spatial regulation of protein degradation also plays an important role during mitosis. Here, we show that the APC/C localizes to centrosomes, the organizers of the eukaryotic microtubule cytoskeleton, specifically during mitosis. The APC/C is recruited to spindle poles by the centrosomal protein Cep152. We not only identify Cep152 as a novel APC/C interaction partner, but also as an APC/C substrate. Importantly, the APC/C-dependent degradation of Cep152 creates a negative feedback loop that controls Cep152 removal from spindle poles during mitosis. We show that persistent Cep152 at the centrosome sequesters Cep57 into a complex and away from pericentrin, thereby inhibiting microtubule nucleation. Thus, our study establishes how the APC/C is recruited to the centrosome, and extends its function from being a critical regulator of mitosis to working as a positive governor of spindle assembly.

Introduction

During mitosis a mother cell divides into two daughter cells that both inherit identical genetic material. This process needs to be tightly controlled to ensure that chromosomes are equally distributed. It is therefore regulated by multiple mechanisms that work together to coordinate a successful cell division. One important regulatory mechanism is ubiquitin-mediated protein degradation, which controls the abundance of different cell cycle regulators during mitosis. The anaphase promoting complex/cyclosome (APC/C) is an E3 ubiquitin ligase governing this process. APC/C activity is coordinated by the correct attachment of chromosomes to the mitotic spindle, promoting the ubiquitin mediated degradation of its target proteins including cyclin B and securin. During recent years the molecular structure and mechanism of the APC/C have been uncovered [1-4], however relatively little is known about the role of its intracellular localization. The APC/C has been observed at kinetochores during an active spindle assembly checkpoint (SAC)[5] and at chromosomes[6]. Additionally, studies suggest that localized protein degradation plays an important role during mitosis. The APC/C substrate cyclin B for example, was reported to be first degraded around spindle poles[7, 8]. Consequently, the APC/C was also shown to localize to spindle poles and this recruitment is dependent on the protein NuMA and the motor protein dynein[9, 10]. However, it is unclear if there are additional proteins that interact with the APC/C at spindle poles that define its localization, or if there are other specific functions which are fulfilled by the APC/C at the centrosome.

Centrosomes are cellular organelles and the major organizers of the microtubule cytoskeleton in eukaryotic cells[11]. They consist of two cylindrical shaped structures named centrioles that are embedded in a protein-rich matrix, the pericentriolar material (PCM). Centrosomes are duplicated in S-phase when each mother centriole gives rise to exactly one new daughter centriole. In mitosis, centrosomes form the centre of spindle poles and

organize the mitotic spindle apparatus[12]. At anaphase, both newly formed daughter cells inherit one centrosome that splits apart in a process called disengagement. They subsequently serve as new mother centrioles during the next duplication cycle[13, 14]. Centrosomes dynamically recruit additional proteins around them to form the PCM, including proteins like pericentrin (PCNT), Cdk5rap2/Cep215 and gamma-tubulin (γTub), that are required for microtubule nucleation[15-19]. The PCM has been shown to increase in size before mitosis[20-23].

In this study we investigate the localization and function of the APC/C at spindle poles. Using a combination of super-resolution and confocal microscopy, cell biology and biochemical assays, we show that during mitosis the APC/C is localized to the PCM, forming a ring-like pattern. We establish that the main interacting protein responsible for the localization of the APC/C to the centrosome is Cep152, which we additionally show to be a novel APC/C substrate. Cep152 is locally ubiquitinated by the APC/C at the centrosome during mitosis, which in turn decreases the localization of the APC/C itself at the centrosome. This negative feedback loop controlling APC/C localization is required for proper assembly of the mitotic spindle. Stabilization of a Cep152 mutant that cannot be targeted by the APC/C results in reduced microtubule nucleation and increased chromosome mis-segregation. This phenotype is caused by sequestering the PCNT-binding protein Cep57 into an inhibitory complex. Once Cep152 is removed from the centrosome by the APC/C, Cep57 is liberated and can recruit PCNT, aiding microtubule nucleation. Hence, our work shows for the first time a role of Cep152 during mitosis and extends the function of the APC/C from being a critical director of cell cycle progression, to additionally also functioning as a positive regulator of mitotic spindle assembly.

Results

The APC/C is a component of the mitotic centrosome

During interphase, the APC/C is localized throughout the cell, with an increased signal present around the centrosome (Extended Data Figure 1a). This localization resembles the pattern of centriolar satellites, small membrane-less granules that surround the centrosome and which were proposed to function as storage for centrosomal proteins[24-26]. Immunofluorescence of the essential satellite component PCM1[27] together with APC2, revealed that the APC/C colocalized with centriolar satellites (Extended Data 1a). This is in agreement with a recent proteomics study of centriolar satellites that also detected the APC/C to be present in these structures[28]. Centriolar satellites are dissolved during mitosis when most of the APC/C signal is localized to the cytoplasm. However, we also detected an accumulation of signal around the spindle poles (Extended Data 1b). To allow for better visualization of the APC/C signal at subcellular structures, we pre-extracted soluble cytoplasmic proteins before fixation of the cells[9]. This allowed us to specifically visualize the APC/C using antibodies against the subunits APC2 and APC3 at the spindle poles (Figure 1a).

It is tempting to speculate that APC/C molecules localized at spindle poles could be part of the centrosome. Indeed, purification of centrosomes from cells that were arrested in mitosis showed co-elution of the APC/C with centrosomal fractions (Figure 1b). Comparison of centrosomes purified from mitotic and interphase cells showed a significant increase in the APC/C signal in the former, indicating that the APC/C localizes to centrosomes specifically in mitosis (Figure 1c, d). Additionally, we also detected the APC/C co-activators Cdc20 and Cdh1, which had previously been found to localize to the spindle poles[29-31]. We also detected BubR1 in centrosomal fractions, but did not observe co-elution of the other SAC proteins Mad2 or Bub3 (Figure 1b). This is in agreement with a previous observation that BubR1

localizes to centrosomes independently of the mitotic checkpoint complex (MCC)[32]. These results raise the interesting possibility that centrosomal APC/C is not inhibited by the MCC.

To determine whether APC/C localization to the centrosome is constant during mitosis, cells were fixed and stained at different time points after entering mitosis. We measured the intensity of the APC/C around the centrosome (marked by γTub) and categorized the cells based on their chromosome alignment and the spindle morphology into three categories. We observed that the APC/C is highly accumulated at the centrosome during prophase, when cells possess mostly a monopolar spindle. With further progression through mitosis (pro-metaphase) the APC/C signal at the centrosome decreases and is undetectable in metaphase (Figure 1e).

The APC/C localizes inside the PCM towards the proximal end of the centriole

To better understand the localization of the APC/C at the centrosome, we performed direct Stochastic Optical Reconstruction Microscopy (dSTORM)[33, 34] of prophase-arrested cells. In two dimensions, the APC/C localizes in a regular, spot-like, circular pattern that is reminiscent of the 9-fold symmetry of centrioles (Figure 2a and Extended Data 2a). The interphase PCM consists of different layers or rings, defined by their diameter. Mitotic PCM is thought to be much more disorganized[20-22]. However, our data suggest that the APC/C persists in a regular pattern, with a ring diameter of 524 +/- 77 nm (Figure 2b). Based on previous measurements, this places the APC/C towards the outer region of the intermediate PCM, close to proteins like Cep152, Cdk5rap2, and PCNT [20, 23]. However, this comparison has to be considered carefully, because previous measurements have only been performed on interphase centrosomes. Using two-colour 3D-STORM the APC/C was observed to accumulate mostly in one plane along the centriolar lumen marker centrin[35, 36] (Figure 2c and Extended Data 2b). Since centrioles are cylindrical in shape, this preferential localization

could indicate that the APC/C is gathered to one end of the structure, either distal or proximal. To address which end, co-staining with the proximal end marker C-NAP1 was performed. C-NAP1 acts as a platform to which the linker protein rootletin is attached, thereby keeping both centrosomes tethered together[37, 38]. While the rootletin linker is resolved in mitosis, some C-NAP1 remains in prophase/pro-metaphase at the centrosome, serving as a proximal end marker[37]. Two-colour 3D STORM showed that the APC/C and C-NAP1 reside within a similar Z-plane (Figure 2d and Extended Data 2c). Interestingly, C-NAP1 forms two distinct dots towards one side of the APC/C ring. We speculate that this might be the side where the daughter centriole is attached. The remaining C-NAP1 could serve as a template to assemble a new rootletin linker in the next cell cycle. Analysis of single centrosomal APC/C dots showed a diameter of 76 +/- 28 nm (Extended Data Figure 2d, 2e), which coincides well with the calculated size of a single APC/C molecule of 35 nm plus two times 15 nm for the primary and secondary antibodies. To test this result, we used human APC/C purified from insect cells and performed dSTORM imaging using the same conditions. The measured diameter in this case was 69 +/- 20 nm (Extended Data Figure 2d - 2f), indicating that the APC/C dots at the centrosome very likely represent only one or a maximum of two APC/C molecules. In conclusion, we show that single APC/C molecules accumulate in a symmetrical ring-like pattern surrounding the proximal end of the centriole within the intermediate PCM (Figure 2e).

The APC/C interacts with several other centrosomal proteins

To determine which protein(s) are responsible for targeting the APC/C to the centrosome, we performed proximity labelling and mass-spectrometry. For this, we tagged the APC/C subunits APC2 and APC3 in independent cell lines with BioID2 under the control of a tetracycline inducible promotor (Extended Data Figure 3a). This improved version[39] of the

biotin ligase BirA is constitutively active. Upon addition of free biotin to cell, the BirA ligase covalently attaches biotin to proteins that are in close proximity to the tagged APC/C subunits. Immunoprecipitation from whole cell lysates using streptavidin confirmed the successful incorporation of the BioID2-tagged APC subunits into the APC/C, as well as the proficient labelling with biotin (Figure 3a). To specifically enrich for centrosomal proteins that interact with the APC/C, we purified centrosomes from our BioID2 cell lines and subsequently performed a streptavidin pulldown (Figure 3b), which was then analysed by mass-spectrometry. Label-free quantification[40] of the different datasets identified several centrosomal proteins that show a strong enrichment in both tagged cell lines (Figure 3c and Extended Data Table 1). These included Cep131, Cep152, Cep170, Cep192, Cep350 and PCM1. Subsequent analysis focussed on the Cep proteins, but not PCM1, since it is the main component of pericentriolar satellites where the APC/C localizes during interphase (Extended Data Figure 1a). However, satellites are dissolved during mitosis, and PCM1 is not localized at the centrosome at this time[41]. It was therefore excluded as being a false positive, probably caused by potential contamination with interphase cells in our sample preparation. Cep152 and Cep192 interact with each other and the localization of Cep152 at centrosomes depends on Cep192[42, 43]among other proteins. Cep131 is a component of pericentriolar satellites, but in contrast to PCM1 localizes to the centrosome during mitosis[44]. Cep131 was also reported to interact with and recruit Cep152 to the centrosome[45]. These three proteins are all localized towards the proximal end of the centriole. Cep170 is localized close to the distal appendages and is involved in organizing the microtubule network[46]. Cep350 (also known as CAP350) directly interacts with and anchors microtubules at the centrosome and the golgi apparatus[47, 48]. Additionally, both proteins were recently found in pericentriolar satellites[28, 49].

To investigate the relationship between the identified proteins and the APC/C, we separately depleted the different Cep proteins (Figure 4a and Extended Data Figure 4a - 4d)

and measured the intensity of the APC/C at the centrosome in mitosis (Figure 4b, 4c). Removal of most Cep proteins resulted in various degrees of reduced APC/C intensity, except for Cep350 where APC/C intensity at the centrosome remained unchanged (Figure 4b, 4c). Subsequent analysis focussed on Cep1321, Cep152, Cep170 and Cep192, excluding Cep350.

Some of the Cep proteins are known to interact with each other or depend on one of the other proteins for their localization[42, 43, 45]. To generate a small-scale interaction network, we measured the intensity of each Cep protein under the depletion conditions of the other proteins (Figure 4e and Extended Data Figure 4a - 4d). Cep131, Cep170 and Cep192 localize independently to the centrosome and did not depend on any of the other proteins. However, Cep152 intensity at the centrosome was reduced in the absence of Cep131 and Cep192 (Extended Data Figure 4b), consistent with previous data[42, 43, 45]. It therefore seems likely that the reduced APC/C intensity upon depletion of Cep131 and Cep192 is a secondary effect due to the absence of Cep152 in these conditions (Figure 4e). Based on these data, indicating that Cep170 appeared to belong to a different interaction network, we excluded Cep170 from further analysis. Immunoprecipitation from cell lines expressing inducible GFP-tagged constructs of Cep131, Cep152, and Cep192 showed that these Cep proteins can interact with the APC/C (Figure 4d), validating our mass-spec data. However, we cannot exclude that these interactions could also be indirect and mediated by the centrosome itself. Additional Cep proteins including Cep57 and Cep63 also form a complex with Cep152[50], as we will discuss later (Figure 4e). In conclusion, Cep152 is the main interacting protein of the APC/C at the centrosome, with smaller contributions from other proteins.

Cep152 is a substrate of the APC/C substrate

Curiously, upon depletion of the APC/C by siRNA, Cep152 intensity at the centrosome was increased (Figure 5a, 5b and Extended Data Figure 5a). This prompted us to investigate whether Cep152 is not only responsible for targeting the APC/C to the centrosome, but is also a substrate of the APC/C. Staining of cells during different stages of mitosis showed that the intensity of Cep152 at the centrosome decreases (Extended Data Figure 5b) in a similar fashion as the APC/C intensity (Figure 1e). Sequence analysis[51] of Cep152 revealed a potential D box and KEN box pair, the recognition motifs of APC/C substrates, present between residues 716 and 742, (Figure 5c). The D box fits the consensus motif and is well conserved in mammals, but not in frog and fish. The KEN box however is modified to a KDN, which is unusual. To corroborate the idea that Cep152 is a potential APC/C substrate, a small peptide that comprises the sequence of Cep152 incorporating the D box/KEN box pair was tested in a ubiquitination-competition assay. Cyclin B1 was incubated with purified APC/C in the presence or absence of either an Hsl1 peptide (incorporating the D box of the strong APC/C substrate Hsl1) or the Cep152 peptide, respectively. Ubiquitination of cyclin B1 is abolished in the presence of the Hsl1 peptide and drastically reduced when the Cep152 peptide is used (Figure 5d). This indicates that the Cep152 peptide can impede the ubiquitination of cyclin B1, consistent with the idea that it contains authentic APC/C degron motifs.

We mutated the potential D box and KEN box individually (referred to as DB and K, respectively) or together (called DBK) and created cell lines that inducibly express eGFP-tagged variants of Cep152 (Extended Data Figure 5c). As before, the localization of eGFP-Cep152 during different mitotic stages was analysed. EGFP-Cep152^{WT} (wild-type) serves as control and behaves as shown for the endogenous protein. Notably, eGFP-Cep152^{DBK} shows an increased centrosomal localization during pro-metaphase and metaphase, compared to eGFP-Cep152^{WT} (Figure 5e). A pool of eGFP-Cep152^{DBK} is still removed from the centrosome between prophase and pro-metaphase, although, not as strongly as the WT protein (Figure

5e). A potential explanation of this observation could be that a subset of Cep152 is re-localized from the centrosome independently of the APC/C and the remaining pool is only then targeted for ubiquitination. Both single mutants, eGFP-Cep152^{DB} and eGFP-Cep152^{K}, showed an increased intensity at the centrosome compared with eGFP-Cep152^{WT}, but not as pronounced as the double mutant eGFP-Cep152^{DBK} (Extended Data Figure 5e). Surprisingly, when cells were released from a G2 arrest into mitosis and samples were probed for total Cep152 via immunoblot, Cep152 levels did not decrease (Extended Data Figure 5c). This suggests that Cep152 ubiquitination by the APC/C is a local event at the centrosome and not throughout the whole cell.

Persistent Cep152 at the centrosome leads to mitotic errors

A mitotic role for Cep152 has not so far been established. Cells expressing eGFP-Cep152^{DBK} exhibited a strong reduction in spindle microtubule intensity compared to cells expressing eGFP-Cep152^{WT} (Figure 6a). Similarly, when the APC/C was depleted from cells, which also leads to the stabilization of Cep152 at the centrosome (Figure 5b), a reduction of microtubule intensity was observed (Figure 5b and Extended Data Figure 5a). Nucleation of microtubules depends on the successful accumulation and expansion of the pericentriolar material (PCM) in mitosis[52, 53]. The PCM includes proteins like PCNT and Cdk5rap2. In the presence of non-degradable eGFP-Cep152^{DBK}, the fluorescence intensities of PCNT and Cdk5rap2 at the centrosome are reduced (Figure 6b, 6c and Extended Data Figure 6a, 6b). This suggests that the PCM does not accumulate to the same degree as in WT cells, resulting in reduced microtubule nucleation. To further test this idea, a cold treatment to depolymerize all microtubules in mitotic cells was performed. After shifting cells back to 37 °C, nucleation of new microtubules from the centrosome can be measured at different time points. In cells expressing eGFP-Cep152^{WT}, microtubules were visible again after 5 min. In

contrast, cells expressing eGFP-Cep152^{DBK} showed both a delay in microtubule nucleation (Figure 6d) and in establishing a bipolar spindle (Extended Data Figure 6d). Based on these data we reasoned that cells expressing eGFP-Cep152^{DBK} would need more time to form a mitotic spindle and complete mitosis. We performed live cell microscopy imaging of cells expressing the different eGFP-Cep152 variants and analysed the time from nuclear envelope breakdown (NEBD) to metaphase, and the time from metaphase to anaphase onset. In cells expressing eGFP-Cep152^{DBK} both phases were prolonged compared to cells with eGFP-Cep152^{WT} or the single mutants (Figure 6e, 6f and Extended Data Figure 6e), consistent with the data that in these cells microtubule nucleation is diminished. An increased time from metaphase to anaphase onset indicates that these cells have problems with correctly or stably attaching their chromosomes to the mitotic spindle, which results in mitotic errors. Consequently, the number of cells that either show mis-aligned chromosomes during metaphase or lagging chromosomes during anaphase (together referred to as “mitotic errors”), was increased in cells expressing eGFP-Cep152^{DBK} (Figure 6g and Extended Data Figure 6f).

The observed phenotypes are reminiscent of Cep57 depletion, which also causes defects in both microtubule nucleation and PCNT recruitment[21, 54]. Because Cep57 forms a complex with Cep63 and Cep152[50] and recruits PCNT to the centrosome[21], we reasoned that in this complex, Cep152 inhibits Cep57 from interacting with PCNT. Removal of Cep152 from the centrosome by the APC/C would therefore allow Cep57 to bind PCNT, enhancing microtubule nucleation. We found that Cep57 levels at the centrosome remain constant throughout mitosis (Extended Data Figure 7a), in contrast to Cep152 and Cep63 which both decrease (Figure 5a, Extended Data Figure 5a, Extended Data Figure 7b). To test our hypothesis directly, we depleted Cep152 and performed an immunoprecipitation of endogenous Cep57 from mitotic cells. In the absence of Cep152 more PCNT is associated

with Cep57 (Figure 6h), consistent with the hypothesis that Cep152 inhibits Cep57 – PCNT interactions.

Discussion

The data presented in this study reveal the crucial role of the APC/C at the centrosome. Recruitment of the APC/C to the centrosome depends on Cep152, which is itself an APC/C substrate. This negative feedback ensures that Cep152 is removed from the centrosome, a step that is important for proper microtubule nucleation (Figure 7a, 7b).

Based on our data we propose that during interphase the APC/C accumulates in centriolar satellites. Previous studies have shown that the APC/C is localized to spindle poles in human cells and that this localization depends on the proteins NuMA and dynein[10], both of which have been implicated in the transport of centriolar satellites[55-57]. Interestingly, some of the identified APC/C interacting proteins are not only components of the centrosome or PCM, but also of centriolar satellites. Indeed, a recent proteomic study identified the APC/C as minor component of centriolar satellites[28]. This opens up the possibility that the APC/C is a dynamic component of centriolar satellites and is thereby transported to the centrosome together with some of its interacting proteins. It also offers an explanation for the Cep170 depletion phenotype that leads to a reduction of APC/C intensity at the centrosome. Cep170 was recently identified as a component of centriolar satellites[28, 49, 58, 59]. Its centrosomal localization was shown to be mainly at the distal end of the mother centriole[46, 60], where it cannot interact with the APC/C which localizes proximally. However, if satellite-localized Cep170 is involved in transporting the APC/C to the centrosome, Cep170 depletion could result in a failure to do so. A similar effect could also contribute to the phenotype of Cep131 depletion where the APC/C is also absent from centrosome. However, in this case a direct

relationship between Cep131 and Cep152 was previously established[45] and confirmed by our study, which we propose to account for the main phenotype.

Once satellites disassemble in mitosis[41] the APC/C localizes to the centrosome inside the PCM. This behaviour is similar to other proteins like PCNT, Cdk5rap2 and γTub, which, as for the APC/C, reside in a similar layer surrounding the centrosome[20, 23]. The main interacting protein of the APC/C at the centrosome is Cep152. Our data show that in the absence of Cep152, APC/C can no longer localize properly to the centrosome. This localization, however, is important, as interfering with the timely removal of Cep152 from centrosomes by the APC/C results in reduced microtubule nucleation and consequently in chromosome alignment and segregation errors. This phenotype is very similar to Cep57 depletion and we established that Cep152 has an inhibitory function on Cep57. In the presence of stabilized Cep152, Cep57 is not released from this inhibition and recruitment of PCNT is hampered.

A function of Cep152 in mitotic spindle assembly has not been previously established, probably because a stabilized Cep152 mutant was not available. Our work, therefore, also implicates Cep152 as an inhibitor of mitotic spindle formation. To ensure timely removal of Cep152 from the centrosome it is locally degraded by the APC/C. This very elegant dual function of Cep152 as a recruiter as well as a substrate of the APC/C ensures that Cep152 is locally and timely degraded at centrosomes and not throughout the cell. This might be important to ensure that enough Cep152 is present during the next S-phase when it is absolutely required for centriole duplication[42, 61].

The Cep152 D box and KEN box pair is unusual, with the Glu (E) of the KEN exchanged to an Asp (D). The KEN motif is important for the Cdh1 mediated ubiquitination of APC/C substrates, but it also involved in the recognition of APC/C^{Cdc20}. Modifications of KEN motifs are very rare, but nonetheless have been reported[62, 63] and it is possible that this could contribute to the avidity of APC/C substrates. For example, the modification of the Cep152

KEN box could contribute to the local degradation at the centrosome, where the APC/C and Cep152 come into close contact, but it would inhibit Cep152 ubiquitination in the cytoplasm. Additionally, Cep152 seems to be a weaker APC/C substrate for example compared to Hsl1, because a Cep152 peptide cannot inhibit cyclin B1 ubiquitination as efficiently as the Hsl1 peptide. Another factor that could have a positive influence on the local Cep152 degradation is the observation that the MCC is absent from the centrosome. This could favour a very rapid activation of the APC/C to ensure that Cep152 is degraded before other substrates, because persistent Cep152 delays microtubule nucleation. The details of the mechanisms responsible for regulating the APC/C localized to centrosomes are not currently understand.

Taken together, our work establishes how the APC/C is recruited to the centrosome and reveals its function to locally degrade Cep152, an inhibitor of mitotic spindle assembly.

Material and Methods

Tissue culture and cell cycle synchronization

HEK293 FlpIn-TRex cells (Invitrogen) were cultured in DMEM (Gibco) supplemented with 10% tetracycline free FBS (PAN Biotech) at 37 °C and 5% CO_2. For the stable integration of eGFP-Cep131, eGFP-Cep192, and eGFP-Cep152 (WT, DB, K, DBK) into the genome the corresponding genes were cloned into the pcDNA5-FRT-TO vector (Invitrogen) with an N-terminal eGFP tag. HEK293 FlpIn-TREX cells were co-transfected with the respective pCDNA5-FRT-TO plasmid and pOG44, containing the flippase, using HBS buffer. Briefly, cells were seeded the evening before transfection and the medium was exchanged the next morning. Both plasmids were mixed with 160 mM $CaCl_2$ and 2x HBS buffer (final concentrations: 137 mM NaCl, 5 mM KCl, 0.7 mM Na_2HPO_4, 7.5 mM D-glucose, 21 mM HEPES) and added to the cells. The next steps were performed according to the Invitrogen

manual. Cells were selected using 100 μg/mL Hygromycin B gold (InVivoGen). For creation of the BioID2-APC2 and APC3-BioID2 cell lines the same protocol was performed, but the pcDNA5-FRT-TO vector was modified to either include an N-terminal or a C-terminal BioID2 tag. All stable cell lines were kept under selection. Protein expression was induced with 250 ng/mL doxycyclin (Sigma). Cell cycle synchronization was performed using a combination of 2.5 mM thymidine (Sigma) to arrest cells in or before S-phase and either 300 nM nocodazole (Sigma) or 500 nM taxol (Sigma) or 5 μM STLC (Sigma) or 10 μM RO-3305 (Santa Cruz) for a mitotic arrest. Cells were released from thymidine after 16 h by washing three times with pre-warmed medium using the same volume as during culture. The second drug was added 4 h after thymidine release and incubated for another 16 h. Release from RO-3306 was performed in the same way.

RNAi mediated protein depletion

Cells were seeded at a density of 50% 16 h before transfection with siRNA. RNAi was performed using RNAiMAX reagent (Invitrogen) according to the manual. For the depletion of all proteins a double depletion protocol using two times 20 nM oligo was used. In short, 16 h after seeding the cells they were transfected with the first round of siRNA and 8 h later thymidine was added (see above). Again 16 h later the cells were released from thymidine and the second round of siRNA transfection was performed. The thymidine block and release were repeated and cells were arrested in mitosis afterwards (see above). This protocol ensures that most of the cells only perform one round of mitosis, which avoids problems with centrosome duplication (in case of the depletion of centrosomal proteins) or cell cycle arrest (in case of APC/C depletion). The following siRNA oligos were used: GL2 AACGUACGCGGAAUACUUCGA[dt][dt], APC6_5 AUGAUGCUCUAGAUAACCGAA[dt][dt], APC6_6 CCCAUGCACUUCGGUCACGAA[dt][dt], APC2_6

CUCACUGGAUCGUAUCUACAA[dt][dt], APC2_5 AAGGUUCUUCUACCGCAUCUA[dt][dt], Cep131 CUGACAACUUGGAGAAAUU[dt][dt], Cep170 GAAGGAAUCCUCCAAGUCA[dt][dt], Cep350 AUGAACGAUAUCAGUGCUAUA[dt][dt], Cep192 AAGGAAGACAUUUUCAUCUCU[dt][dt], Cep152 GCGGAUCCAACUGGAAAUCUA[dt][dt]

Immunoblotting

For immunoblotting about 3 x 10^6 cells / mL were washed once with PBS, spun down and resuspended in NuPAGE LDS Sample Buffer (Invitrogen). After heating the solution for 5 min at 95 °C, five to ten microliters were loaded on to a Novex Bis-Tris 4% - 12% gel (Invitrogen) and run for the appropriate time. The proteins were transferred to a nitrocellulose membrane (GE Healthcare), which was blocked with 5% dried milk in PBS-Tx (PBS, 0.1% Triton-X 100). The primary antibodies were incubated over night at 4 °C, the secondary antibodies were used for 1 h at room temperature. The following antibodies were used for immunoblotting: pericentrin (Abcam ab4448, 1:2000), APC8 (Abcam ab182003 1:1000), APC6 (Cell Signaling 9499, 1:1000), APC3 (Cell Signaling 12530, 1:1000), APC2 (Cell Signaling 12301, 1:1000), CDH1 (Abcam ab89535, 1:1000), BubR1 (Abcam ab54894, 1:500), Mad2(Abcam ab10691, 1:1000), APC3 (Sigma C7104, 1:500), gamma-tubulin (Sigma T6557, 1:1000), beta-actin (Santa Cruz sc-47778-HRP, 1:2000), alpha-Tubulin (BioRad MCA78G, 1:2000), Cdc20 (Santa Cruz sc-8358, 1:100), Bub3 (BD 811730, 1:500), Cep131 / AZI-1 (Bethyl A301-415A, 1:1000), Cep170 (Abcam ab72505, 1:500), Cep350 (Novus NB100-59811, 1:500), Cep152 (Bethyl A302-480A, 1:500), Cep192 (Bethyl A302-324A, 1:1000), Cyclin B1 (Abcam ab72, 1:1000), His (Takara/Clontech 631212, 1:1000), GFP (Roche 11814460001, 1:1000), Cep57 (Genetex GTX115931, 1:1000), secondary anti-rabbit (Thermofisher 31462, 1:10.000), secondary anti-mouse (Agilent P0260, 1:10.000), secondary anti-rat (Santa Cruz 2032, 1:10.000).

Immunoprecipitation

HEK cells were treated with siRNA as described above and lysed in IP-buffer (150 mM NaCl, 1 mM $MgCl_2$, 50 mM HEPES pH 8, 1 mM EGTA, 0.5% Triton-X 100, complete protease inhibitors (Roche)) for 30 min on ice. The lysate was centrifuged for 10 min at 15.000 g at 4 °C and the supernatant was carefully taken off. Subsequently, it was incubated with 5 μg Cep57 antibody (Genetex) or normal rabbit IgG (Cell Signaling) coupled to magnetic protein G beads (Invitrogen) for 3 h at 4 °C under constant agitation. The beads were washed three times with lysis buffer and eluted by cooking in NuPAGE LDS Sample Buffer (Invitrogen) with 5 mM DTT.

Live cell microscopy

A SP8 confocal microscope (Leica) equipped with a heated environmental chamber, an argon laser, a 630 nm laser line and an APO CS2 40x/1.1 water immersion lens was used for live cell imaging. Live cell microscopy was performed as described before[64]. The imaged cells were analysed for the time of NEBD, the time when a metaphase plate was observed for the first time and the time of anaphase onset. Mitotic errors that were visible during the movies were noted down and analysed as well.

Immunofluorescence microscopy and antibodies

After cells were grown in tissue culture plates, mitotic cells were collected by a gentle wash with medium and spun down onto polylysine (Sigma) treated cover glasses for 5 min at 650 g. Cells were fixed using either methanol or formaldehyde. Except for Figure 6 and Extended Data Figure S1 cells were always pre-extracted for 2 min at 37 °C using 0.2% Triton-X 100 in

PHEM buffer (60 mM Pipes, 25 mM Hepes, 10 mM EGTA, 2 mM $MgCl_2$, pH 7.5). For methanol, cells were incubated for 5 min at –20 °C with pre-cooled methanol. Afterwards cells were rehydrated with PBS and washed with PBS-Tx, before blocking with ABDIL (1% BSA, 0.1% Triton-X 100, PBS). For formaldehyde, cells were incubated two times for 5 min at 37 °C with pre-warmed 3.7% formaldehyde in PHEM buffer. Subsequently cells were washed in PBS-Tx and blocked in ABDIL. Primary antibody incubation was performed for 1 h at room temperature. After washing three times with ABDIL, the secondary antibodies were incubated for 1 h at room temperature, and washed again three times in ABDIL. If microtubules were stained, the process was repeated with an alpha-tubulin antibody (BioRad MCA78G, 1:2000) to minimize cross reaction. In the last washing step 1 μg/mL DAPI (Sigma) was included. Primary antibodies used for staining were: pericentrin (Abcam ab4448, 1:2000), APC2 (Cell Signaling 12301, 1:1000), APC3 (sigma C7104, 1:500), gamma-Tubulin (sigma T6557, 1:1000), Cep131 / AZI-1 (Bethyl A301-415A, 1:1000), Cep170 (Abcam ab72505, 1:500), Cep350 (Novus NB100-59811, 1:500), Cep152 (Bethyl A302-480A, 1:500), Cep192 (Bethyl A302-324A, 1:1000), GFP (Abcam ab6556, 1:1000), Centrin3 (Novus H00001070-M01, 1:1000), Cep57 (Genetex GTX115931, 1:500). Secondary antibodies were pre-absorbed and Alexafluor coupled from Thermofisher. Alexa-488, Alexa-568, and Alexa-647 were used in all combinations against mouse, rabbit, or rat primary antibodies.

Images were acquired with an SP8 confocal microscope (Leica) quipped with 405 nm, 488 nm, 568 nm and 633 nm laser lines using an APO CS2 63x/1.4 oil immersion objective. Image resolution was set to 1024x1024 with an 3x zoom-in, 600 Hz scan speed and 2x line average. A Z-spacing of 0.23 mm was always used. Laser powers and detector gain were set for each primary antibody individually, but were kept constant between different experiments with the same antibody to ensure reproducibility.

Image quantification and statistical analysis

Fluorescent images were analysed with ImageJ. Maximum intensity projections were created and a circular region of interest was used for the measurements. This could either be a small circle in case of centrosomes or a circle including the whole cell in case of tubulin measurements; the background was measured outside the cells. The integrated density was corrected for the area and the background. All values for the control condition in each experiment were averaged and this mean value was used to normalize all other conditions against the control using Excel (Microsoft). The normalized values were exported to Prism 8 (Graphpad) and plotted. All boxplots display the 5% to 95% range (whiskers), the 25% and 75% range (box) and the median (line). Bar graphs display the mean +/- standard deviation. Statistical analysis was performed in Prism 8 and the tests that were used are described in the corresponding figures legends. All experiments were repeated at least twice using biological replicates.

2D and 3D dSTORM

Direct-STORM was performed with a Nikon N-STORM equipped with 405 nm, 488 nm, 561 nm and 647 nm laser lines (Agilent/Keysight MLC 4008) using an APO TIRF 100x/1.49 oil immersion objective. Cells were cultured in an 8-well glass bottom slide (Ibidi) and fixed and stained as described above. The secondary antibodies used were coupled to Alexafluor-568 or Alexaflour-647 and were additionally fixed with 4% formaldehyde after the staining was concluded (post fix). Before imaging, the wells were incubated for 5 min with Tetraspeck Beads (Thermofisher, 1:100) and subsequently washed with PBS. The cells were imaged in switching buffer (100 U glucose oxidase (Sigma), 10.000 U catalase (Sigma), 8% glucose, 100 mM MEA (Sigma), pH 7.6) by filling the well of the ibidi slide to the top and covering it with a cover glass avoiding air bubbles. For 3D imaging a cylindrical lens was inserted into the light

path. STORM was performed by inducing and observing blinking events of the Alexafluor secondary antibodies, usually 50.000 frames with 10 ms exposure were recorded. Pre- and post-STORM widefield images were acquired as well. Point fitting in 2D and 3D space was performed within the Nikon software. For 2D STORM the resulting images were directly saved from the Nikon software. For 3D STORM the fitted point coordinates were exported, transformed in ImageJ using ChriSTORM and imported using the ThunderSTORM ImageJ plugin. If necessary, two-colour images were manually aligned using the Tetraspeck beads as reference points with the "Align RGB planes" plugin in ImageJ. A gaussian normalization algorithm was used for visualization and the data were rendered in 3D using the ImageJ 3D viewer.

Centrosome purification

Mitotic centrosomes were purified from 2 x 10^8 HEK293 cells. Cells were synchronized with thymidine and nocodazole (see above). One h before harvesting the cells 1 μg/mL Cytochalasin D (sigma) was added. Mitotic cells were collected by shake off and gentle washing with medium. All subsequent steps were performed at 4 °C. Cells were washed once in PBS, once in 0.1x PBS + 8% sucrose and once in 8% sucrose in H_20. The cells were resuspended in 10 mL lysis buffer (1 mM Pipes, 0.1 mM EGTA, 0.1% 2-mercaptoethanol, 0.5% Triton-X 100, EDTA-free complete protease inhibitors (Roche)) and incubated for 10 min. The lysate was centrifuged at 2500 g for 10 min and the supernatant filtered through a 40 μm cell strainer. From a 50x stock of PE (500 mM Pipes, 50 mM EGTA, pH 7.2) the respective volume to prepare a 1x solution was added to the supernatant. Sucrose solutions with 70% (w/v), 60% (w/v), 50% (w/v), and 40% (w/v) were prepared in 1x PE. The cell lysate was carefully layered over 1 mL 60% sucrose cushion in a thin walled Beckman tube (344058) and centrifuged at 10,000 g for 30 min using a slow deceleration. About 70% of the

tube content was removed from the top and discarded and the remaining volume was mixed with the 60% sucrose cushion to get solution of about 20% sucrose. In parallel, a sucrose gradient consisting of 2 mL 70% sucrose (bottom), 1.2 mL 50% sucrose (middle) and 1.2 mL 40% sucrose (top) was prepared in a Beckman tube (344060). The cell lysate containing 20% sucrose was layered over the sucrose gradient and centrifuged for 16 h at 100,000 g using a no break deceleration. The tube with the gradient was pierced at the bottom with an 18G needle and fractions of the following sizes were collected: F1-3 each 500 μL, F4-9 each 200 μL, F10-11 each 500 μL, F12-13 each 1 mL. Centrosome containing fractions were snap frozen in liquid nitrogen.

To prepare samples for mass-spectrometry, cells were treated as described above, but additionally incubated with 50 μM for 24 h before harvesting. After centrosomes were purified, all fractions from the corresponding cell lines were combined and diluted with three times to volume of lysis buffer plus 0.1% SDS. The solution was sonificated using a microtip with the following settings: 1min time, 10 seconds on, 20 seconds off, 45% power. The sonified centrosomes were incubated with magnetic streptavidin beads (MyOne Streptavidin C1, ThermoFisher) over night. Washing was performed one time each in the following order: lysis buffer, SDS buffer (2% SDS in H_2O), salt buffer (500 mM NaCl, 1% Triton-X 100, 1 mM EDTA, 50 mM HEPES, pH 7.6), Tris buffer (50 mM Tris, 50 mM NaCl, pH 7.6). Purified proteins were eluted from the streptavidin beads with Tris buffer plus 5 mM biotin. The whole samples were run on a NuPAGE SDS gel, stained with InstantBlue (Expedeon) and the each lane was cut into 10 equally sized pieces, which were send to mass-spectrometric analysis as described before[4].

Ubiquitination assays

In vitro ubiquitination was performed using APC/C and Cdc20 purified from insect cells. 60 nM APC/C, 30 nM Cdc20, 90 nM UBA1, 300 nM UbcH10, 300 nM Ube2S, 35 μM ubiquitin, 1 μM cyclin B1, 5 mM ATP, 10 mM $MgCl_2$, were mixed in a buffer containing 40 mM HEPES (pH 8.0), 80 mM NaCl, 0.6 mM DTT. The reaction was mixed either with peptides or buffer as control. The Hsl1 peptide has been published before (ref), the Cep152 peptide has the sequence: LQLRSELDKLNKEVTAVQECYLEVCREKDNLEL. The reaction was incubated for 30 min at 23 °C and stopped by the addition of one volume of 2x concentrated NuPAGE LDS loading buffer.

Acknowledgements

We thank F. Gergely from the Cancer Research UK Cambridge Institute for antibodies and discussions. M. van Breugel from the MRC LMB for plasmids containing several Cep proteins. The authors also thank J. Howe from the MRC LMB Light Microscopy for help with STORM, F. Begum from the MRC LMB Mass-Spectrometry for performing the BioID mass-spec runs and S. Zhang for providing components and purified APC/C for in vitro ubiquitination assays. This work was supported by the Medical Research Council (MC_UP_1201/6) and a Cancer Research UK grant (C576/A14109) to D. Barford.

Author Contributions

TT performed and analysed all experiments. JY purified proteins. TT and DB planned experiments and wrote the manuscript.

Competing Interests statement

The authors declare no conflict of interest.

Data availability

All data related to this study is presented within the manuscript and the supporting files. Cell lines that were generated for and used in this study are available upon request from the authors.

References

1. Alfieri, C. *et al.* Molecular basis of APC/C regulation by the spindle assembly checkpoint. *Nature* **536**, 431-436 (2016).
2. Baker, D.J., Dawlaty, M.M., Galardy, P. & van Deursen, J.M. Mitotic regulation of the anaphase-promoting complex. *Cell Mol Life Sci* **64**, 589-600 (2007).
3. Chang, L., Zhang, Z., Yang, J., McLaughlin, S.H. & Barford, D. Atomic structure of the APC/C and its mechanism of protein ubiquitination. *Nature* **522**, 450-454 (2015).
4. Zhang, S. *et al.* Molecular mechanism of APC/C activation by mitotic phosphorylation. *Nature* **533**, 260-264 (2016).
5. Acquaviva, C., Herzog, F., Kraft, C. & Pines, J. The anaphase promoting complex/cyclosome is recruited to centromeres by the spindle assembly checkpoint. *Nature cell biology* **6**, 892-898 (2004).
6. Sivakumar, S., Daum, J.R., Tipton, A.R., Rankin, S. & Gorbsky, G.J. The spindle and kinetochore-associated (Ska) complex enhances binding of the anaphase-promoting complex/cyclosome (APC/C) to chromosomes and promotes mitotic exit. *Molecular biology of the cell* **25**, 594-605 (2014).
7. Huang, J. & Raff, J.W. The disappearance of cyclin B at the end of mitosis is regulated spatially in Drosophila cells. *The EMBO journal* **18**, 2184-2195 (1999).
8. Clute, P. & Pines, J. Temporal and spatial control of cyclin B1 destruction in metaphase. *Nature cell biology* **1**, 82-87 (1999).
9. Tugendreich, S., Tomkiel, J., Earnshaw, W. & Hieter, P. CDC27Hs colocalizes with CDC16Hs to the centrosome and mitotic spindle and is essential for the metaphase to anaphase transition. *Cell* **81**, 261-268 (1995).
10. Ban, K.H. *et al.* The END network couples spindle pole assembly to inhibition of the anaphase-promoting complex/cyclosome in early mitosis. *Developmental cell* **13**, 29-42 (2007).
11. Gonczy, P. Towards a molecular architecture of centriole assembly. *Nature reviews. Molecular cell biology* **13**, 425-435 (2012).
12. Varmark, H. Functional role of centrosomes in spindle assembly and organization. *Journal of cellular biochemistry* **91**, 904-914 (2004).
13. Nigg, E.A. & Holland, A.J. Once and only once: mechanisms of centriole duplication and their deregulation in disease. *Nature reviews. Molecular cell biology* (2018).

14. Stearns, T. Centrosome duplication. a centriolar pas de deux. *Cell* **105**, 417-420 (2001).
15. Kim, J., Kim, J. & Rhee, K. PCNT is critical for the association and conversion of centrioles to centrosomes during mitosis. *Journal of cell science* **132** (2019).
16. Kim, S. & Rhee, K. Importance of the CEP215-pericentrin interaction for centrosome maturation during mitosis. *PloS one* **9**, e87016 (2014).
17. Gupta, G.D. & Pelletier, L. Centrosome Biology: Polymer-Based Centrosome Maturation. *Current biology : CB* **27**, R836-R839 (2017).
18. Thawani, A., Kadzik, R.S. & Petry, S. XMAP215 is a microtubule nucleation factor that functions synergistically with the gamma-tubulin ring complex. *Nature cell biology* **20**, 575-585 (2018).
19. Wieczorek, M. *et al.* Asymmetric Molecular Architecture of the Human gamma-Tubulin Ring Complex. *Cell* **180**, 165-175 e116 (2020).
20. Sonnen, K.F., Schermelleh, L., Leonhardt, H. & Nigg, E.A. 3D-structured illumination microscopy provides novel insight into architecture of human centrosomes. *Biol Open* **1**, 965-976 (2012).
21. Watanabe, K., Takao, D., Ito, K.K., Takahashi, M. & Kitagawa, D. The Cep57-pericentrin module organizes PCM expansion and centriole engagement. *Nature communications* **10**, 931 (2019).
22. Woodruff, J.B., Wueseke, O. & Hyman, A.A. Pericentriolar material structure and dynamics. *Philosophical transactions of the Royal Society of London. Series B, Biological sciences* **369** (2014).
23. Lawo, S., Hasegan, M., Gupta, G.D. & Pelletier, L. Subdiffraction imaging of centrosomes reveals higher-order organizational features of pericentriolar material. *Nature cell biology* **14**, 1148-1158 (2012).
24. Lopes, C.A. *et al.* Centriolar satellites are assembly points for proteins implicated in human ciliopathies, including oral-facial-digital syndrome 1. *Journal of cell science* **124**, 600-612 (2011).
25. Hori, A. & Toda, T. Regulation of centriolar satellite integrity and its physiology. *Cell Mol Life Sci* **74**, 213-229 (2017).
26. Prosser, S.L. & Pelletier, L. Centriolar satellite biogenesis and function in vertebrate cells. *Journal of cell science* **133** (2020).
27. Kubo, A., Sasaki, H., Yuba-Kubo, A., Tsukita, S. & Shiina, N. Centriolar satellites: molecular characterization, ATP-dependent movement toward centrioles and possible involvement in ciliogenesis. *The Journal of cell biology* **147**, 969-980 (1999).
28. Gheiratmand, L. *et al.* Spatial and proteomic profiling reveals centrosome-independent features of centriolar satellites. *The EMBO journal* **38**, e101109 (2019).
29. Kallio, M.J., Beardmore, V.A., Weinstein, J. & Gorbsky, G.J. Rapid microtubule-independent dynamics of Cdc20 at kinetochores and centrosomes in mammalian cells. *The Journal of cell biology* **158**, 841-847 (2002).
30. Zhou, Y., Ching, Y.P., Chun, A.C. & Jin, D.Y. Nuclear localization of the cell cycle regulator CDH1 and its regulation by phosphorylation. *The Journal of biological chemistry* **278**, 12530-12536 (2003).
31. Meghini, F. *et al.* Targeting of Fzr/Cdh1 for timely activation of the APC/C at the centrosome during mitotic exit. *Nature communications* **7**, 12607 (2016).
32. Izumi, H. *et al.* BubR1 localizes to centrosomes and suppresses centrosome amplification via regulating Plk1 activity in interphase cells. *Oncogene* **28**, 2806-2820 (2009).
33. Rust, M.J., Bates, M. & Zhuang, X. Sub-diffraction-limit imaging by stochastic optical reconstruction microscopy (STORM). *Nat Methods* **3**, 793-795 (2006).

34. Betzig, E. *et al.* Imaging intracellular fluorescent proteins at nanometer resolution. *Science* **313**, 1642-1645 (2006).
35. Paoletti, A., Moudjou, M., Paintrand, M., Salisbury, J.L. & Bornens, M. Most of centrin in animal cells is not centrosome-associated and centrosomal centrin is confined to the distal lumen of centrioles. *Journal of cell science* **109 (Pt 13)**, 3089-3102 (1996).
36. Fong, C.S., Kim, M., Yang, T.T., Liao, J.C. & Tsou, M.F. SAS-6 assembly templated by the lumen of cartwheel-less centrioles precedes centriole duplication. *Developmental cell* **30**, 238-245 (2014).
37. Hardy, T. *et al.* Multisite phosphorylation of C-Nap1 releases it from Cep135 to trigger centrosome disjunction. *Journal of cell science* **127**, 2493-2506 (2014).
38. Bahe, S., Stierhof, Y.D., Wilkinson, C.J., Leiss, F. & Nigg, E.A. Rootletin forms centriole-associated filaments and functions in centrosome cohesion. *The Journal of cell biology* **171**, 27-33 (2005).
39. Kim, D.I. *et al.* An improved smaller biotin ligase for BioID proximity labeling. *Molecular biology of the cell* **27**, 1188-1196 (2016).
40. Zybailov, B. *et al.* Statistical analysis of membrane proteome expression changes in Saccharomyces cerevisiae. *J Proteome Res* **5**, 2339-2347 (2006).
41. Kubo, A. & Tsukita, S. Non-membranous granular organelle consisting of PCM-1: subcellular distribution and cell-cycle-dependent assembly/disassembly. *Journal of cell science* **116**, 919-928 (2003).
42. Sonnen, K.F., Gabryjonczyk, A.M., Anselm, E., Stierhof, Y.D. & Nigg, E.A. Human Cep192 and Cep152 cooperate in Plk4 recruitment and centriole duplication. *Journal of cell science* **126**, 3223-3233 (2013).
43. Kim, T.S. *et al.* Hierarchical recruitment of Plk4 and regulation of centriole biogenesis by two centrosomal scaffolds, Cep192 and Cep152. *Proceedings of the National Academy of Sciences of the United States of America* **110**, E4849-4857 (2013).
44. Staples, C.J. *et al.* The centriolar satellite protein Cep131 is important for genome stability. *Journal of cell science* **125**, 4770-4779 (2012).
45. Kodani, A. *et al.* Centriolar satellites assemble centrosomal microcephaly proteins to recruit CDK2 and promote centriole duplication. *eLife* **4** (2015).
46. Guarguaglini, G. *et al.* The forkhead-associated domain protein Cep170 interacts with Polo-like kinase 1 and serves as a marker for mature centrioles. *Molecular biology of the cell* **16**, 1095-1107 (2005).
47. Yan, X., Habedanck, R. & Nigg, E.A. A complex of two centrosomal proteins, CAP350 and FOP, cooperates with EB1 in microtubule anchoring. *Molecular biology of the cell* **17**, 634-644 (2006).
48. Hoppeler-Lebel, A. *et al.* Centrosomal CAP350 protein stabilises microtubules associated with the Golgi complex. *Journal of cell science* **120**, 3299-3308 (2007).
49. Quarantotti, V. *et al.* Centriolar satellites are acentriolar assemblies of centrosomal proteins. *The EMBO journal* **38**, e101082 (2019).
50. Lukinavicius, G. *et al.* Selective chemical crosslinking reveals a Cep57-Cep63-Cep152 centrosomal complex. *Current biology : CB* **23**, 265-270 (2013).
51. Jehl, P., Manguy, J., Shields, D.C., Higgins, D.G. & Davey, N.E. ProViz-a web-based visualization tool to investigate the functional and evolutionary features of protein sequences. *Nucleic Acids Res* **44**, W11-15 (2016).
52. Gould, R.R. & Borisy, G.G. The pericentriolar material in Chinese hamster ovary cells nucleates microtubule formation. *The Journal of cell biology* **73**, 601-615 (1977).
53. Woodruff, J.B. *et al.* The Centrosome Is a Selective Condensate that Nucleates Microtubules by Concentrating Tubulin. *Cell* **169**, 1066-1077 e1010 (2017).

54. Wu, Q. *et al.* Cep57, a NEDD1-binding pericentriolar material component, is essential for spindle pole integrity. *Cell Res* **22**, 1390-1401 (2012).
55. Merdes, A., Ramyar, K., Vechio, J.D. & Cleveland, D.W. A complex of NuMA and cytoplasmic dynein is essential for mitotic spindle assembly. *Cell* **87**, 447-458 (1996).
56. Engelender, S. *et al.* Huntingtin-associated protein 1 (HAP1) interacts with the p150Glued subunit of dynactin. *Human molecular genetics* **6**, 2205-2212 (1997).
57. Merdes, A., Heald, R., Samejima, K., Earnshaw, W.C. & Cleveland, D.W. Formation of spindle poles by dynein/dynactin-dependent transport of NuMA. *The Journal of cell biology* **149**, 851-862 (2000).
58. Gupta, G.D. *et al.* A Dynamic Protein Interaction Landscape of the Human Centrosome-Cilium Interface. *Cell* **163**, 1484-1499 (2015).
59. Barenz, F. *et al.* Ccdc61 controls centrosomal localization of Cep170 and is required for spindle assembly and symmetry. *Molecular biology of the cell*, mbcE18020115 (2018).
60. Mazo, G., Soplop, N., Wang, W.J., Uryu, K. & Tsou, M.F. Spatial Control of Primary Ciliogenesis by Subdistal Appendages Alters Sensation-Associated Properties of Cilia. *Developmental cell* **39**, 424-437 (2016).
61. Brown, N.J., Marjanovic, M., Luders, J., Stracker, T.H. & Costanzo, V. Cep63 and cep152 cooperate to ensure centriole duplication. *PloS one* **8**, e69986 (2013).
62. Castro, A., Vigneron, S., Bernis, C., Labbe, J.C. & Lorca, T. Xkid is degraded in a D-box, KEN-box, and A-box-independent pathway. *Molecular and cellular biology* **23**, 4126-4138 (2003).
63. He, J. *et al.* Insights into degron recognition by APC/C coactivators from the structure of an Acm1-Cdh1 complex. *Molecular cell* **50**, 649-660 (2013).
64. Zhang, S., Tischer, T. & Barford, D. Cyclin A2 degradation during the spindle assembly checkpoint requires multiple binding modes to the APC/C. *Nature communications* **10**, 3863 (2019).

Figure Legends

Fig 1: The APC/C is a component of the mitotic centrosome

a, Mitotic HEK293 cells were pre-extracted, fixed in ice cold methanol (left) or formaldehyde (right) and stained with the indicated antibodies. Scale bars are 5 μm in the overview and 1 μm in the inset. **b**, Centrosomes were purified from mitotic cells using a sucrose gradient. The eluted fractions were immunoblotted against the indicated proteins. The top shows PCNT and γTub as centrosomal proteins, the middle shows several APC/C components and MCC proteins are shown at the bottom. **c**, Centrosomes were purified in parallel from interphase cells and mitotic cells using a sucrose gradient. The first elution fractions were blotted against PCNT as a centrosomal marker and APC3. **d**, Centrosomes from **c** were fixed on a coverglass and stained with the indicated antibodies. The intensity of the APC/C was measured and normalized against the signal intensity on interphase centrosomes (right). **e**, Cells were treated according to the time line (top) and stained against the indicated proteins. The fluorescence intensity of APC2 was measured and normalized against the intensity in prophase. Scale bars are 5 μm in the overview and 1 μm in the inset. N = 77 (prophase), 130 (pro-metaphase), 73 (metaphase). ****$P < 0.0001$ using a simple one-way ANOVA test with Dunnett's multiple comparison.

Fig 2: The APC/C localizes inside the PCM towards the proximal end of the centriole

a, HEK293 cells were arrested in prophase using taxol, pre-extracted and fixed with formaldehyde. APC2 was stained and dSTORM imaging was performed. The merged image shows the diffraction limited widefield image and the reconstructed dSTORM image. The numbers on the dSTORM image indicate the number of APC/C complexes

that can be counted. Scale bars are 5 μm in the overview and 0.5 μm in the inset. **b**, The average diameter of the APC/C rings shown in **a** was measured in at least two directions per centrosome. N = 20. **c, d**, Cells were treated as described in **a**, but additionally stained against the indicated proteins. Two-colour 3D STORM was performed using a cylindrical lens and by imaging both channels sequentially. Three different views are shown. The illustrations below the images indicate the possible orientation of the centrioles. See also Extended Data movies 1 and 2. **e**, A model of the APC/C localization around the centrosome. The APC/C localizes within the PCM towards the proximal end of the centriole.

Fig 3: The APC/C is in close proximity to several other centrosomal proteins

a, HEK293 FlpIn T-Rex cells were treated with tetracycline to induce expression of the stably integrated BioID2 constructs and with or without biotin for proximity labelling. Whole cell lysates were subjected to streptavidin pulldown to enrich for biotinylated proteins. The input and the eluted fractions were immunoblotted against the indicated proteins. **b**, Cells were treated as in **a**, but additionally blocked in mitosis by nocodazole, and mitotic centrosomes were purified via a sucrose gradient. The first elution fractions were immunoblotted against γTubulin as a centrosome marker and the APC/C (left). The centrosome containing fractions were pooled and subsequently used for a streptavidin pulldown to enrich specifically for biotinylated centrosomal proteins (right). **c**, The streptavidin pulldown from **b** was subjected to mass-spectrometry and the data were evaluated by label free analysis. The plots indicate centrosomal proteins with red dots and known APC/C interacting proteins with green dots. Proteins that were chosen for further analysis are indicated the graphs. See Extended Data Table 1 for the full mass-spec dataset.

Fig 4: Depletion of centrosomal proteins leads to loss of the APC/C from the centrosome

a, HEK293 cells were depleted of the centrosomal proteins chosen for further analysis using siRNA. STLC arrested, mitotic whole cell lysates were immunoblotted against the indicated proteins. Actin serves as a loading control. **b**, Cells were treated as in **a** and stained with the indicated proteins. **c**, Quantification of the APC/C intensity at the centrosome from cells shown in **b**. The intensity was normalized against the siGL2 control. N = 140 (siGL2), 109 (siCep131), 52 (siCep152), 86 (siCep70), 51 (siCep192), 63 (siCep350). ****P < 0.0001 using a simple one-way ANOVA test with Dunnett's multiple comparison. **d**, HEK293 FlpIn T-Rex cells stably expressing the indicated eGFP proteins were subjected to a GFP pulldown and blotted against the indicated proteins. Since eGFP-Cep192 was not visible in the GFP immunoblot an additional anti-Cep192 blot was performed. **e**, Interaction model of the different centrosomal proteins with each other and with the APC/C.

Fig 5: Cep152 is a substrate of the APC/C

a, HEK293 cells were depleted of APC2 or APC6 using siRNA and the whole cell lysate was blotted against the indicated proteins. Tubulin serves as a loading control. **b**, STLC arrested mitotic cells were depleted as in **a** and stained against the indicated protein (left). The fluorescence intensity of Cep152 at the centrosome was measured and normalized against the GL2 control. N = 60 (siGL2), 60 (siAPC2), 62 (siAPC6). ***P = 0.0002, ****P < 0.0001 using a simple one-way ANOVA test with Dunnett's multiple comparison. **c**, multiple sequence alignment of the Cep152 potential D-box and KEN. **d**, HEK293 FlpIn T-Rex cell lines expressing eGFP-Cep152 wildtype (WT) or D-box/KEN (DBK) mutant proteins were treated as shown in **Fig 1e** and stained against the indicated proteins (left). The fluorescence intensity of eGFP-Cep152 at the centrosome

was measured and normalized against the intensity of prophase cells of the corresponding cell line (right). N = 44 (WT, prophase), 34 (DBK, prophase), 41 (WT, pro-metaphase), 61 (DBK, pro-metaphase), 33 (WT, metaphase), 38 (DBK, metaphase). ***P = 0.0005, ****P < 0.0001 using a Mann-Whitney U-test. **e**, Cyclin B1 was ubiquitinated in vitro using purified APC/C in the presence or absence of Hsl1 or Cep152 peptide, respectively.

Fig 6: Persistent Cep152 at the centrosome leads to mitotic errors

a, HEK293 FlpIn T-Rex cell lines expressing eGFP-Cep152 wildtype (WT) or D-box/KEN (DBK) mutant proteins were treated as shown in **Fig 1e** and stained against the indicated proteins (left). The fluorescence intensity of tubulin was measured in the whole cell and normalized against the eGFP-Cep152^{WT} cell line (right). N = 78 (WT), 77 (DBK). ****P < 0.0001 using a simple one-way ANOVA test with Dunnett's multiple comparison. **b**, The fluorescence intensity of PCNT at the centrosome in cells from **a** was measured and normalized against the eGFP-Cep152^{WT} cell line. N = 158 (WT), 154 (DBK). ****P < 0.0001 using a simple one-way ANOVA test with Dunnett's multiple comparison. **c**, HEK293 FlpIn T-Rex cell lines expressing eGFP-Cep152 wildtype (WT) or D box/KEN box (DBK) mutant proteins were treated as in **a** and stained against the indicated proteins (left). The fluorescence intensity of Cdk5rap2 was measured at the centrosome and normalized against the eGFP-Cep152^{WT} cell line (right). N = 174 (WT), 179 (DBK). *P = 0.024 using a Mann-Whitney U-test. **d**, HEK293 FlpIn T-Rex cell lines expressing eGFP-Cep152 wildtype (WT) or D box/KEN box (DBK) mutant proteins were subjected to 45 min at 4 °C. Cells were fixed at the indicated times after shifting them back to 37 °C and stained against tubulin (left). The fluorescent intensity of tubulin was measured in the whole cell at the 30 min after shifting cells back to 37 °C and normalized against the eGFP-Cep152^{WT} cell line (right). N = 61 (WT), 66 (DBK). ****P <

0.0001 using a simple one-way ANOVA test with Dunnett's multiple comparison. **e**, eGFP-Cep152^{WT} and eGFP-Cep152^{DBK} cell lines were subjected to live cell imaging. Exemplary still images from the movies are shown. See Extended Data Movie 5 and 6. Nuclear envelope breakdown (NEBD), metaphase and anaphase onset are marked. DNA was stained with SiR-DNA. Unaligned chromosomes are indicated with yellow arrows. **f**, Cells from **e** were analysed for the time they need to progress from NEBD to metaphase (NEBD – Meta) and from metaphase to anaphase onset (Meta – Ana). Bar graphs show the mean +/- SEM. ***P = 0.0006 using a simple one-way ANOVA test with Dunnett's multiple comparison. N = 4 experiments, WT = 197 cells, DBK = 189 cells. **g**, Cells from **e** were analyzed for misaligned chromosomes during metaphase and lagging chromosomes during anaphase, combined as mitotic errors. Bar graphs show the mean +/- SEM. ***P = 0.0005 using a Holm-Sidak t-test. N = 4 experiments. **h**, HEK cells were treated with control siRNA (siGL2) or siRNA against Cep152 (siCep152) and lysed for anti-Cep57 immunoprecipitation. The eluates were probed against for the indicated proteins by immunoblotting.

Fig 7: Model for APC/C regulation of mitotic spindle assembly through Cep152

a, Interaction network between the APC/C and the identified centrosomal proteins. The main APC/C interacting protein at the centrosome is Cep152, which is also an APC/C substrate creating a negative feedback loop. **b**, Model of microtubule nucleation in the presence of wild type (top) or stabilized (bottom) Cep152.

Figure 1

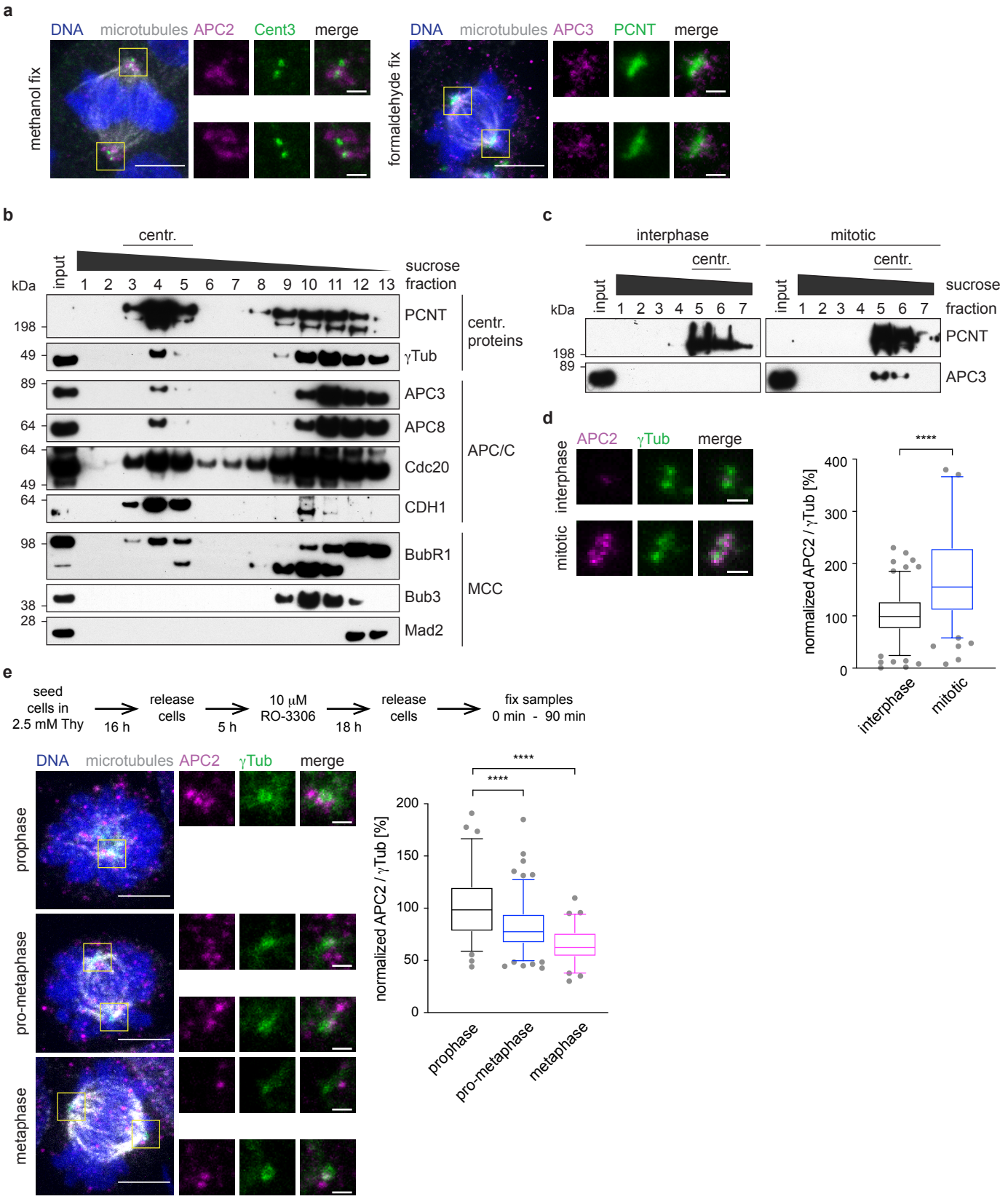
a
DNA
microtubules
APC2
Cent3
merge
methanol fix
DNA
microtubules
APC3
PCNT
merge
formaldehyde fix
b
centr.
input
1 2 3 4 5 6 7 8 9 10 11 12 13
sucrose fraction
kDa
198
49
89
64
64
49
64
98
38
28
PCNT
γTub
APC3
APC8
Cdc20
CDH1
BubR1
Bub3
Mad2
centr. proteins
APC/C
MCC
c
interphase
mitotic
centr.
centr.
input
1 2 3 4 5 6 7
sucrose fraction
kDa
198
89
PCNT
APC3
d
APC2
γTub
merge
interphase
mitotic
normalized APC2 / γTub [%]
400
300
200
100
0
****
interphase
mitotic
e
seed cells in 2.5 mM Thy
16 h
release cells
5 h
10 µM RO-3306
18 h
release cells
fix samples 0 min - 90 min
DNA
microtubules
APC2
γTub
merge
prophase
pro-metaphase
metaphase
normalized APC2 / γTub [%]
200
150
100
50
0
****
****
prophase
pro-metaphase
metaphase

Figure 2

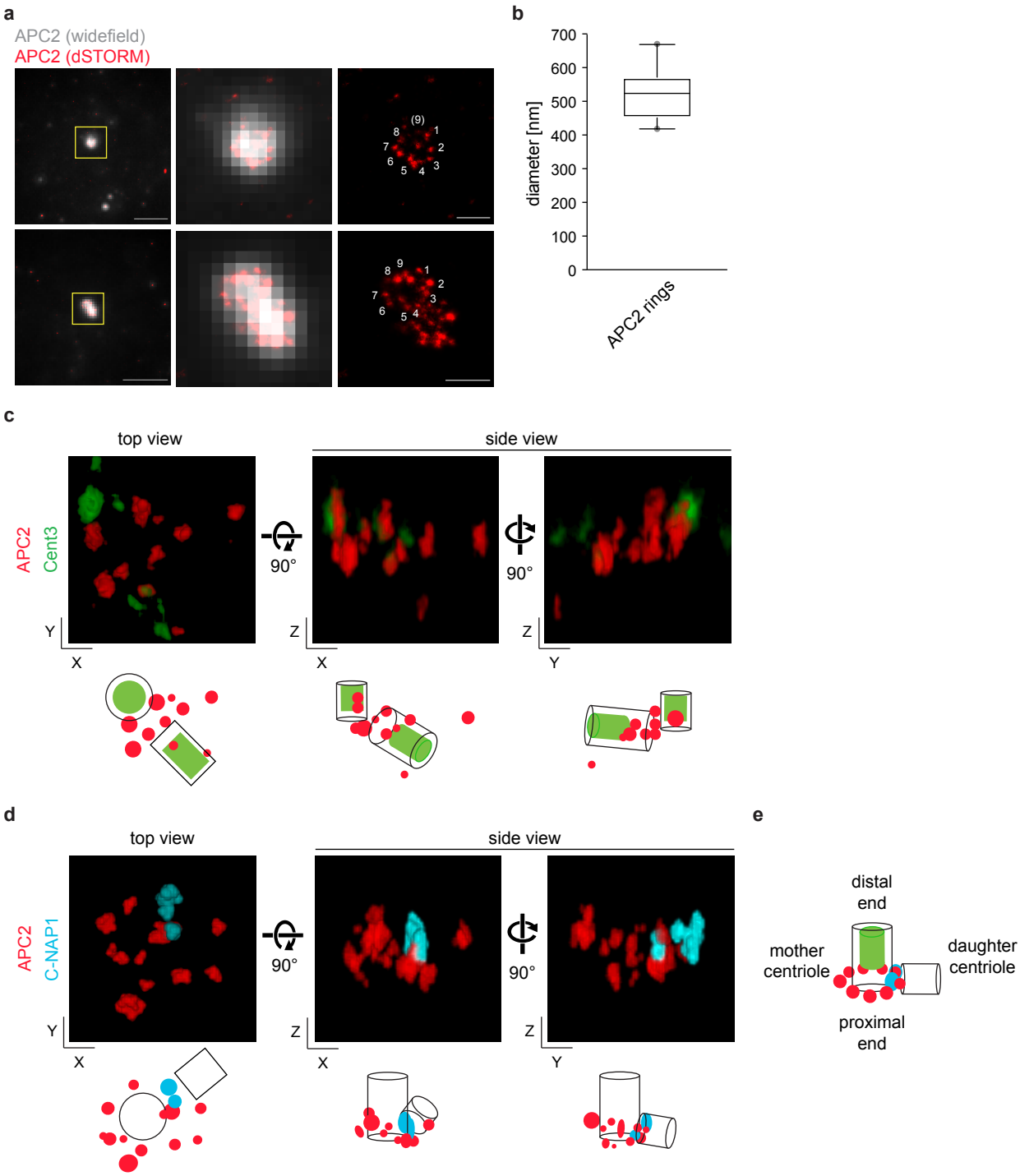
a
APC2 (widefield)
APC2 (dSTORM)
(9)
1
2
3
4
5
6
7
8
9
b
diameter [nm]
700
600
500
400
300
200
100
0
APC2 rings
c
top view
side view
APC2
Cent3
90°
90°
Y
X
Z
X
Z
Y
d
top view
side view
APC2
C-NAP1
90°
90°
Y
X
Z
X
Z
Y
e
distal
end
mother
centriole
daughter
centriole
proximal
end

Figure 3

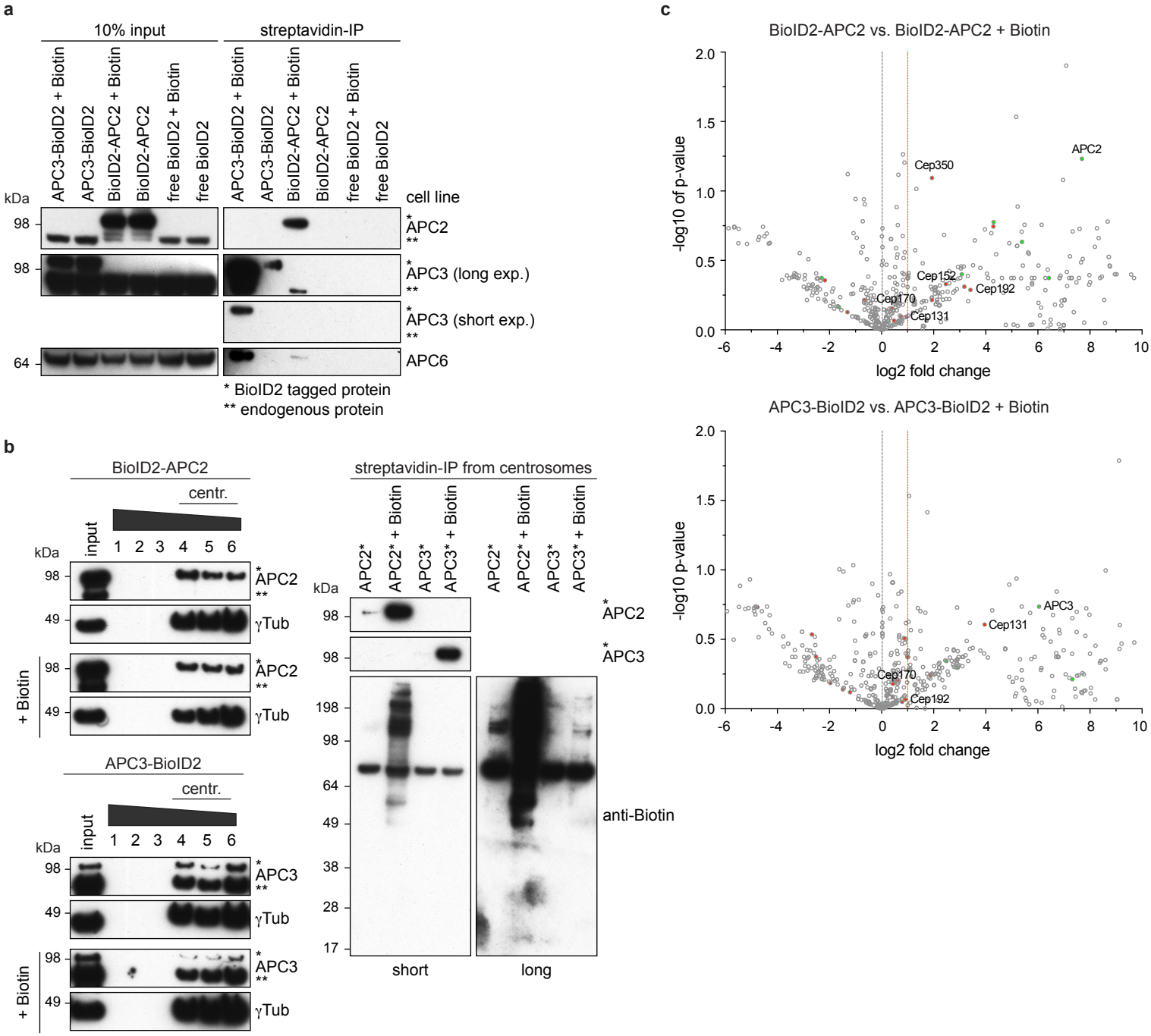
a
10% input
streptavidin-IP
APC3-BioID2 + Biotin
APC3-BioID2
BioID2-APC2 + Biotin
BioID2-APC2
free BioID2 + Biotin
free BioID2
cell line
kDa
98
64
*APC2
**
*APC3 (long exp.)
**
*APC3 (short exp.)
**
APC6
* BioID2 tagged protein
** endogenous protein
b
BioID2-APC2
centr.
input
1 2 3 4 5 6
kDa
98
49
*APC2
**
γTub
+ Biotin
APC3-BioID2
*APC3
streptavidin-IP from centrosomes
APC2*
APC2* + Biotin
APC3*
APC3* + Biotin
198
64
38
28
17
anti-Biotin
short
long
c
BioID2-APC2 vs. BioID2-APC2 + Biotin
-log10 of p-value
log2 fold change
APC2
Cep350
Cep152
Cep192
Cep170
Cep131
APC3-BioID2 vs. APC3-BioID2 + Biotin
APC3
Cep131
Cep170
Cep192

Figure 4

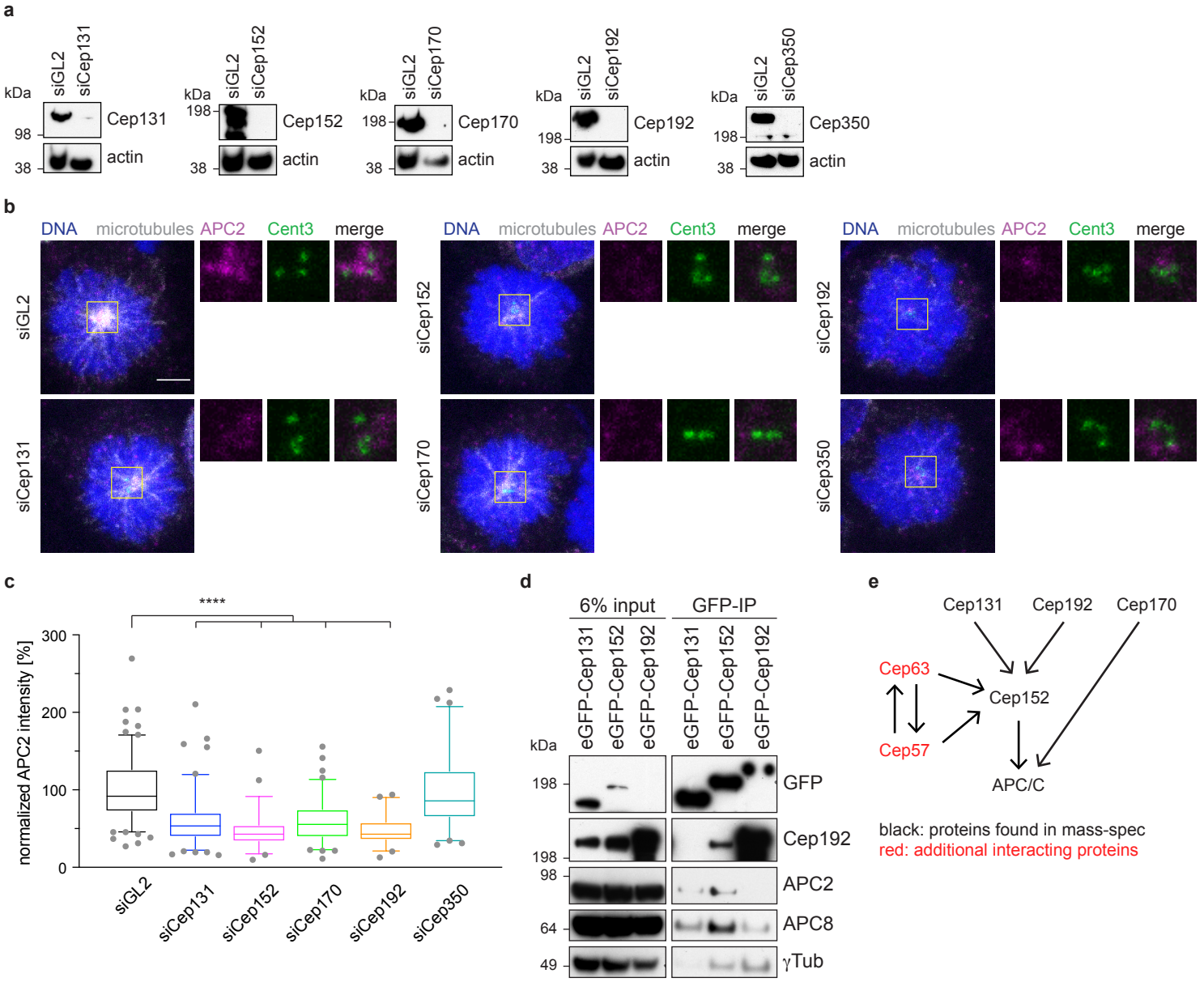
a
kDa
siGL2
siCep131
Cep131
actin
98
38
siCep152
Cep152
198
siCep170
Cep170
siCep192
Cep192
siCep350
Cep350
b
DNA
microtubules
APC2
Cent3
merge
siGL2
siCep131
siCep152
siCep170
siCep192
siCep350
c
****
normalized APC2 intensity [%]
300
200
100
0
siGL2
siCep131
siCep152
siCep170
siCep192
siCep350
d
6% input
GFP-IP
eGFP-Cep131
eGFP-Cep152
eGFP-Cep192
kDa
198
GFP
Cep192
98
APC2
64
APC8
49
γTub
e
Cep131
Cep192
Cep170
Cep63
Cep152
Cep57
APC/C
black: proteins found in mass-spec
red: additional interacting proteins

Figure 5

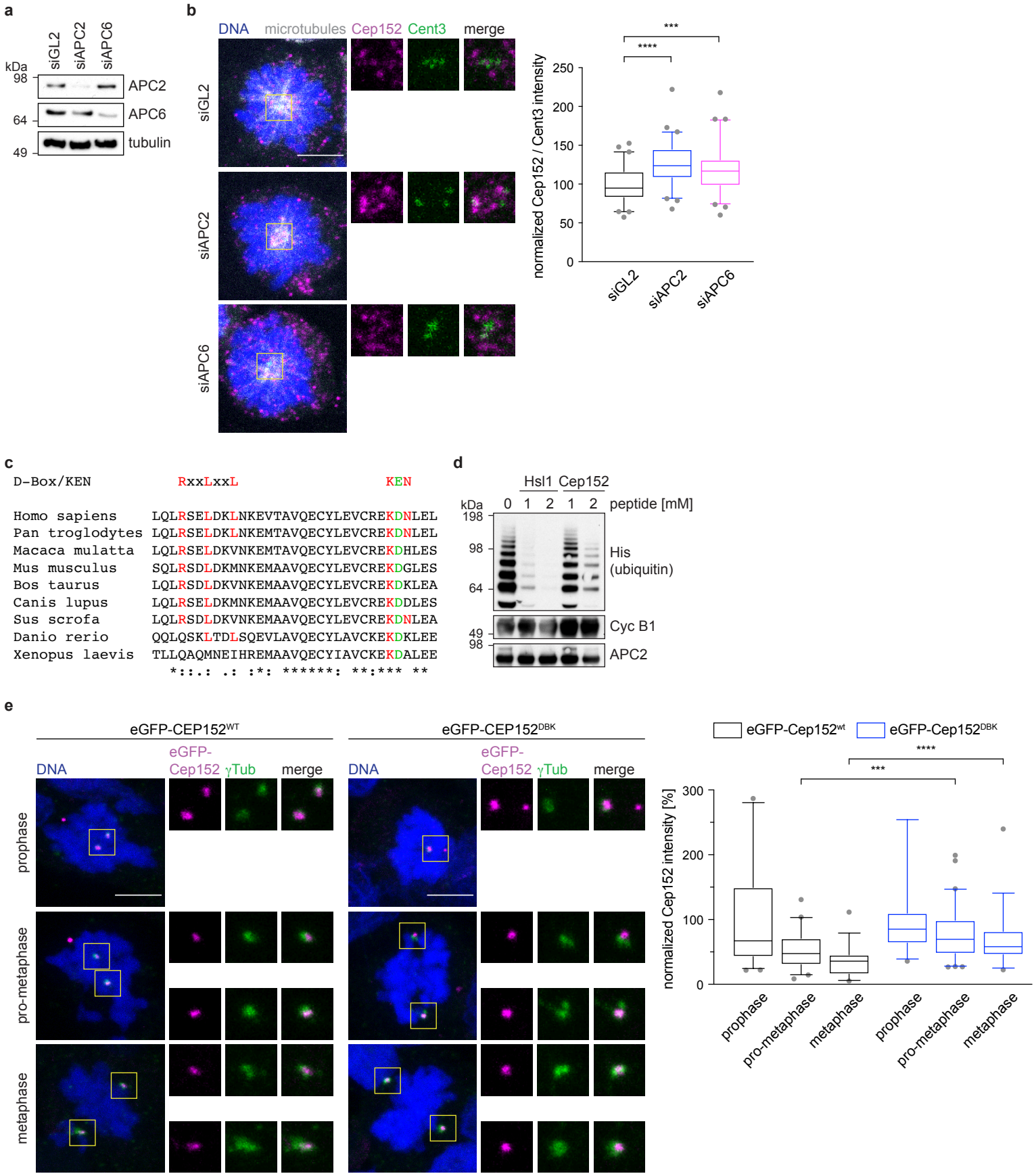
a
siGL2
siAPC2
siAPC6
kDa
98
64
49
APC2
APC6
tubulin
b
DNA
microtubules
Cep152
Cent3
merge
siGL2
siAPC2
siAPC6
normalized Cep152 / Cent3 intensity
250
200
150
100
50
0
***
****
siGL2
siAPC2
siAPC6
c
D-Box/KEN RxxLxxL KEN
Homo sapiens LQLRSELDKLNKEVTAVQECYLEVCREKDNLEL
Pan troglodytes LQLRSELDKLNKEMTAVQECYLEVCREKDNLEL
Macaca mulatta LQLRSELDKVNKEMTAVQECYLEVCREKDHLES
Mus musculus SQLRSDLDKMNKEMAAVQECYLEVCREKDGLES
Bos taurus LQLRSDLDKVNKEMAAVQECYLEVCREKDKLEA
Canis lupus LQLRSELDKMNKEMAAVQECYLEVCREKDDLES
Sus scrofa LQLRSDLDKVNKEMAAVQECYLEVCREKDNLEA
Danio rerio QQLQSKLTDLSQEVLAVQECYLAVCKEKDKLEE
Xenopus laevis TLLQAQMNEIHREMAAVQECYIAVCKEKDALEE
:::.: .: :: ******: **:*** **
d
Hsl1
Cep152
kDa
0 1 2 1 2 peptide [mM]
198
98
64
49
98
His (ubiquitin)
Cyc B1
APC2
e
eGFP-CEP152WT
eGFP-CEP152DBK
DNA
eGFP-Cep152
γTub
merge
prophase
pro-metaphase
metaphase
eGFP-Cep152wt
eGFP-Cep152DBK
normalized Cep152 intensity [%]
300
200
100
0
***
****
prophase
pro-metaphase
metaphase
prophase
pro-metaphase
metaphase

Figure 6

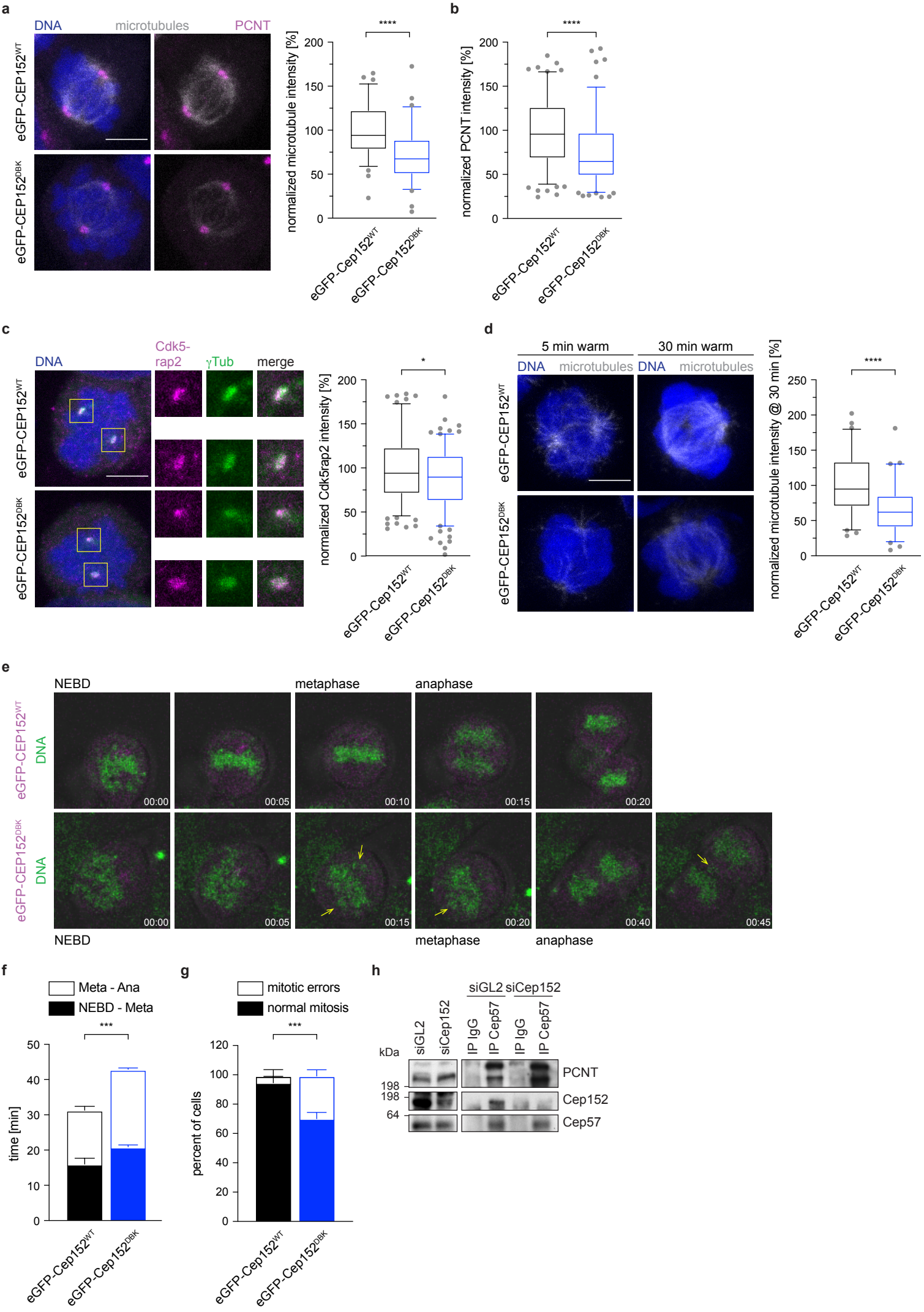
a
DNA
microtubules
PCNT
eGFP-CEP152WT
eGFP-CEP152DBK
normalized microtubule intensity [%]
****
eGFP-Cep152WT
eGFP-Cep152DBK
b
normalized PCNT intensity [%]
****
c
DNA
Cdk5-rap2
γTub
merge
normalized Cdk5rap2 intensity [%]
*
d
5 min warm
30 min warm
normalized microtubule intensity @ 30 min [%]
****
e
NEBD
metaphase
anaphase
00:00
00:05
00:10
00:15
00:20
00:40
00:45
f
Meta - Ana
NEBD - Meta
time [min]
***
g
mitotic errors
normal mitosis
percent of cells
***
h
siGL2
siCep152
IP IgG
IP Cep57
kDa
PCNT
Cep152
Cep57
198
64

Figure 7

a

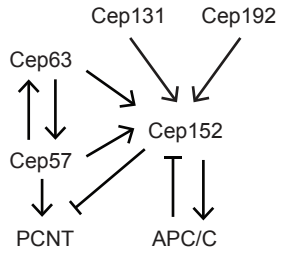
Cep131
Cep192
Cep63
Cep152
Cep57
PCNT
APC/C

b

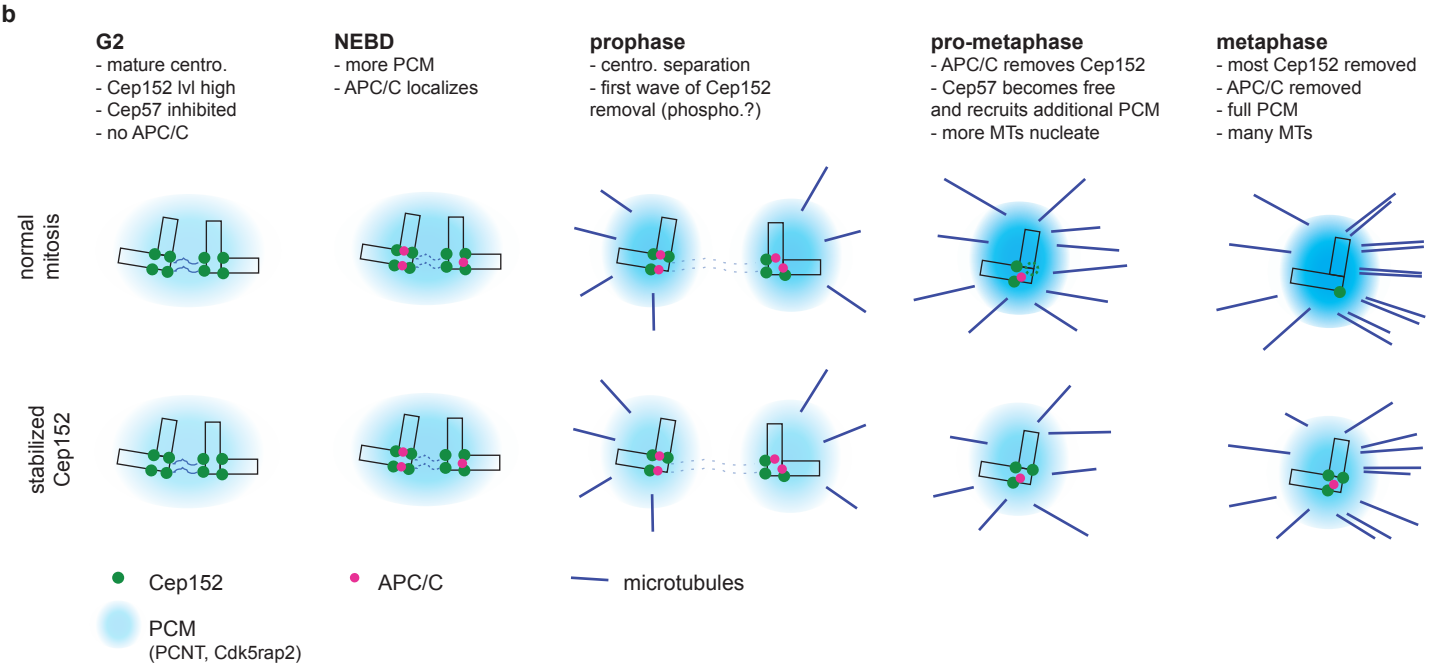
G2
- mature centro.
- Cep152 lvl high
- Cep57 inhibited
- no APC/C
NEBD
- more PCM
- APC/C localizes
prophase
- centro. separation
- first wave of Cep152 removal (phospho.?)
pro-metaphase
- APC/C removes Cep152
- Cep57 becomes free and recruits additional PCM
- more MTs nucleate
metaphase
- most Cep152 removed
- APC/C removed
- full PCM
- many MTs
normal mitosis
stabilized Cep152
Cep152
APC/C
microtubules
PCM
(PCNT, Cdk5rap2)

Extended Data Figure 1

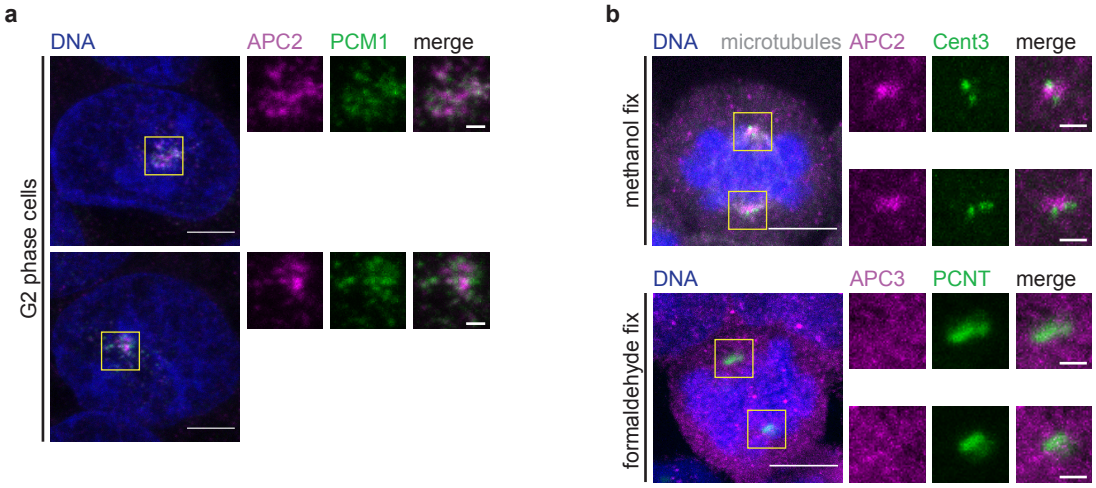

The APC/C localizes to centriolar satellites in interphase. a, HEK293 cells were release from a thymidine arrest for 4 hours, fixed with ice colde methanol and stained with the indicated antibodies. Scale bars are 5 µm in the overview and 1 µm in the inset. **b**, Mitotic HEK293 cells were not pre-extracted, fixed in ice cold methanol (top) or formaldehyde (bottom) and stained with the indicated antibodies. Scale bars are 5 µm in the overview and 1 µm in the inset.

Extended Data Figure 2

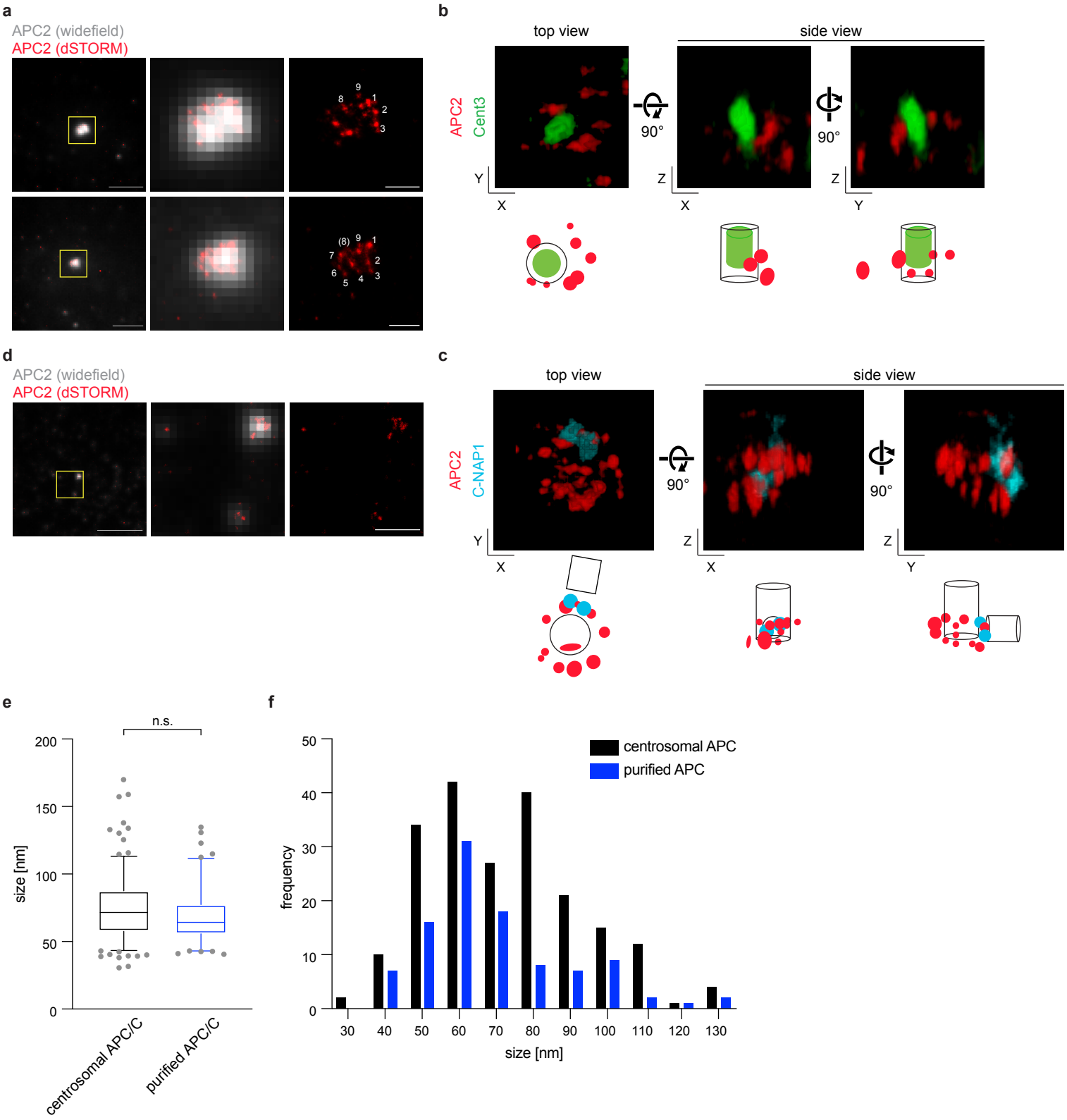

dSTORM imaging of the APC/C at mitotic centrosomes. a, Additional images, related to Figure 2a. HEK293 cells were arrested in prophase using taxol, pre-extracted and fixed with formaldehyde. APC2 was stained and dSTORM imaging was performed. The merged image shows the diffraction limited widefield image and the reconstructed dSTORM image. The numbers on the dSTORM image indicate the number of APC/C complexes that can be counted. Scale bars are 5 µm in the overview and 0.5 µm in the inset. **b**, **c**, Additional images, related to Figure 2c,d. Cells were treated as described in **a**, but additionally stained against the indicated proteins. Two-color 3D STORM was performed using a cylindrical lens and by imaging both channels sequentially. Three different views are shown. The illustrations below the images indicate the possible orientation of the centrioles. See also Supplementary movies 3 and 4. **d**, Purified APC/C was fixed with formaldehyde. APC2 was stained and dSTORM imaging was performed. The merged image shows the diffraction limited widefield image and the reconstructed dSTORM image. Scale bars are 5 µm in the overview and 0.5 µm in the inset. **e**, The average diameter of the signal dots measured after STORM imaging of centrosomal APC/C or purified APC/C. N = 212 (centrosomal APC/C), 101 (purified APC/C). **f**, frequency distribution of the data presented in **d**.

Extended Data Figure 3

a

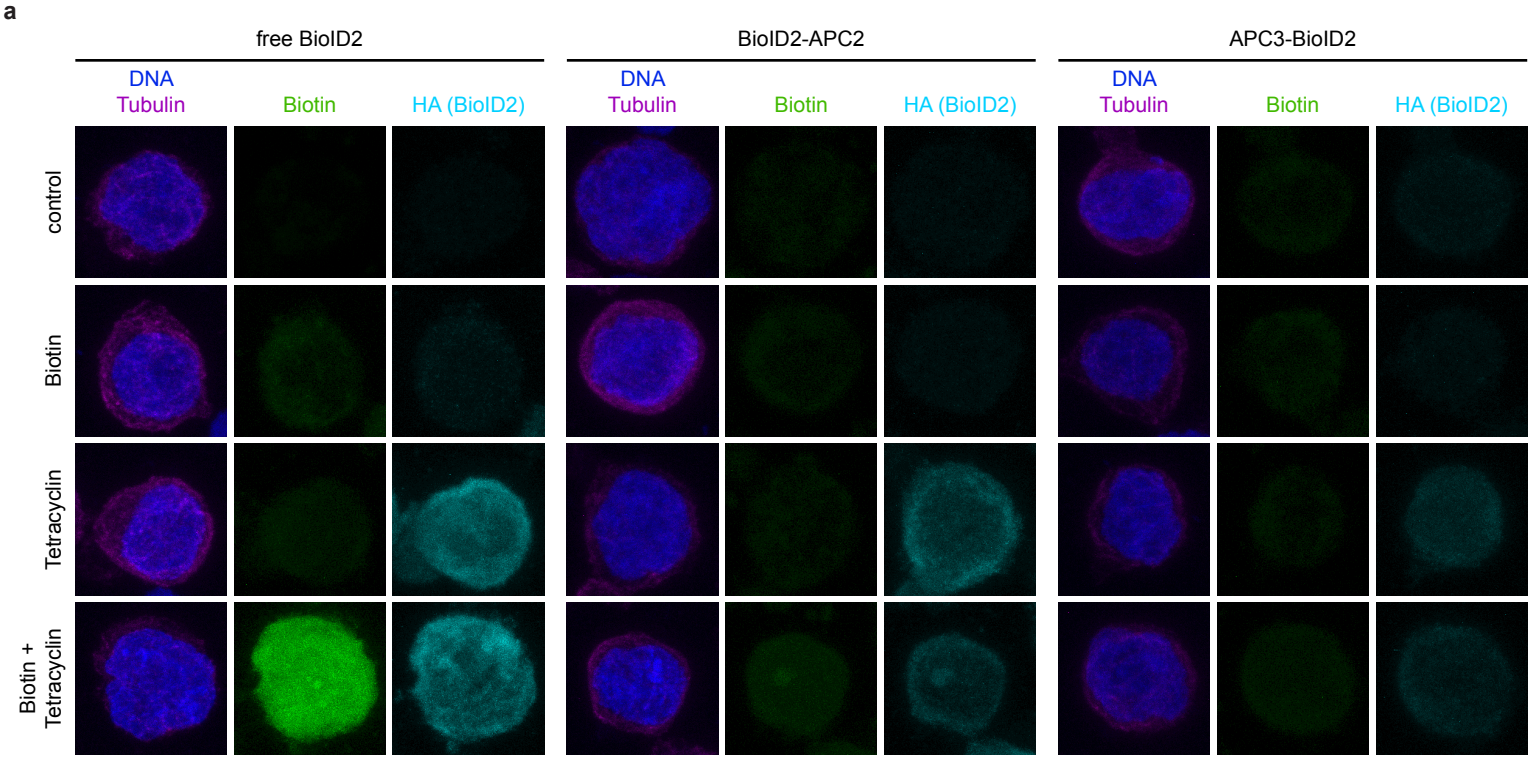

APC/C subunits tagged with BioID2 biotinylate soluable proteins. a, Flp-In T-Rex HEK293 cells with stable integration of the indicated constructs were treated with theindicated compounds. Tetracycline induces the expression of the transgene and Biotin is ligated to target proteins in close proximity to the BioID2 biotin ligase only if the transgene is expressed.

Extended Data Figure 4

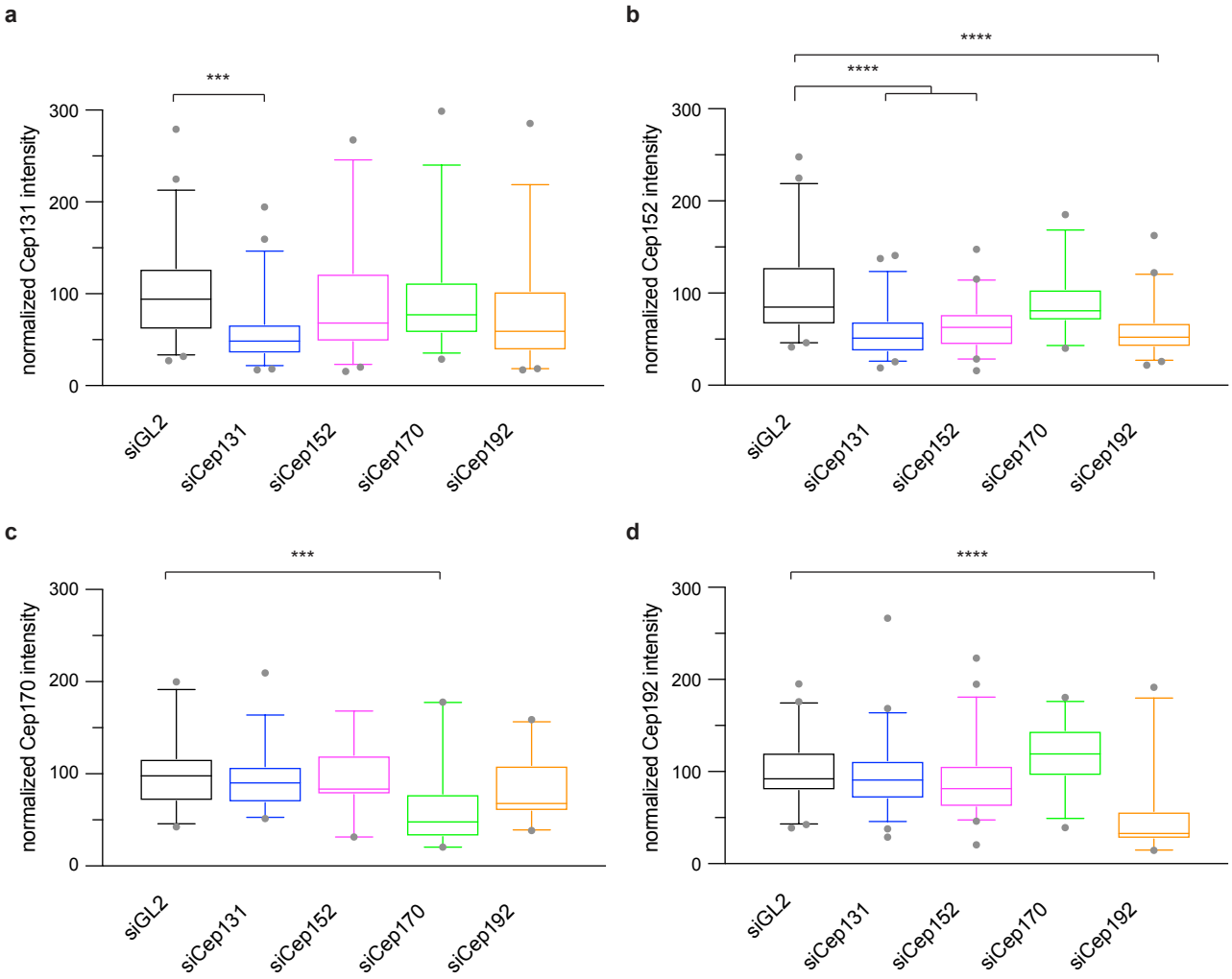

Depletion and cross-staining of centrosomal proteins identified by BioID2 mass-spectrometry. a, **b**, **c**, **d**, HEK293 cells were depleted of the indicated centrosomal proteins using siRNA and arrested in mitosis by STLC. Cells were stained with the indicated antibodies and the centrosomal signal of each protein was quantified. The intensity was normalized against the siGL2 control. ****P < 0.0001 and ***P < 0.001 using a simple one-way ANOVA test with Dunnett's multiple comparison. **a**, N = 48 (siGL2), 57 (siCep131), 49 (siCep152), 37 (siCep70), 39 (siCep192). **b**, N = 51 (siGL2), 50 (siCep131), 40 (siCep152), 29 (siCep70), 50 (siCep192). **c**, N = 29 (siGL2), 33 (siCep131), 19 (siCep152), 29 (siCep70), 22 (siCep192). **d**, N = 51 (siGL2), 46 (siCep131), 44 (siCep152), 33 (siCep70), 38 (siCep192).

Extended Data Figure 5

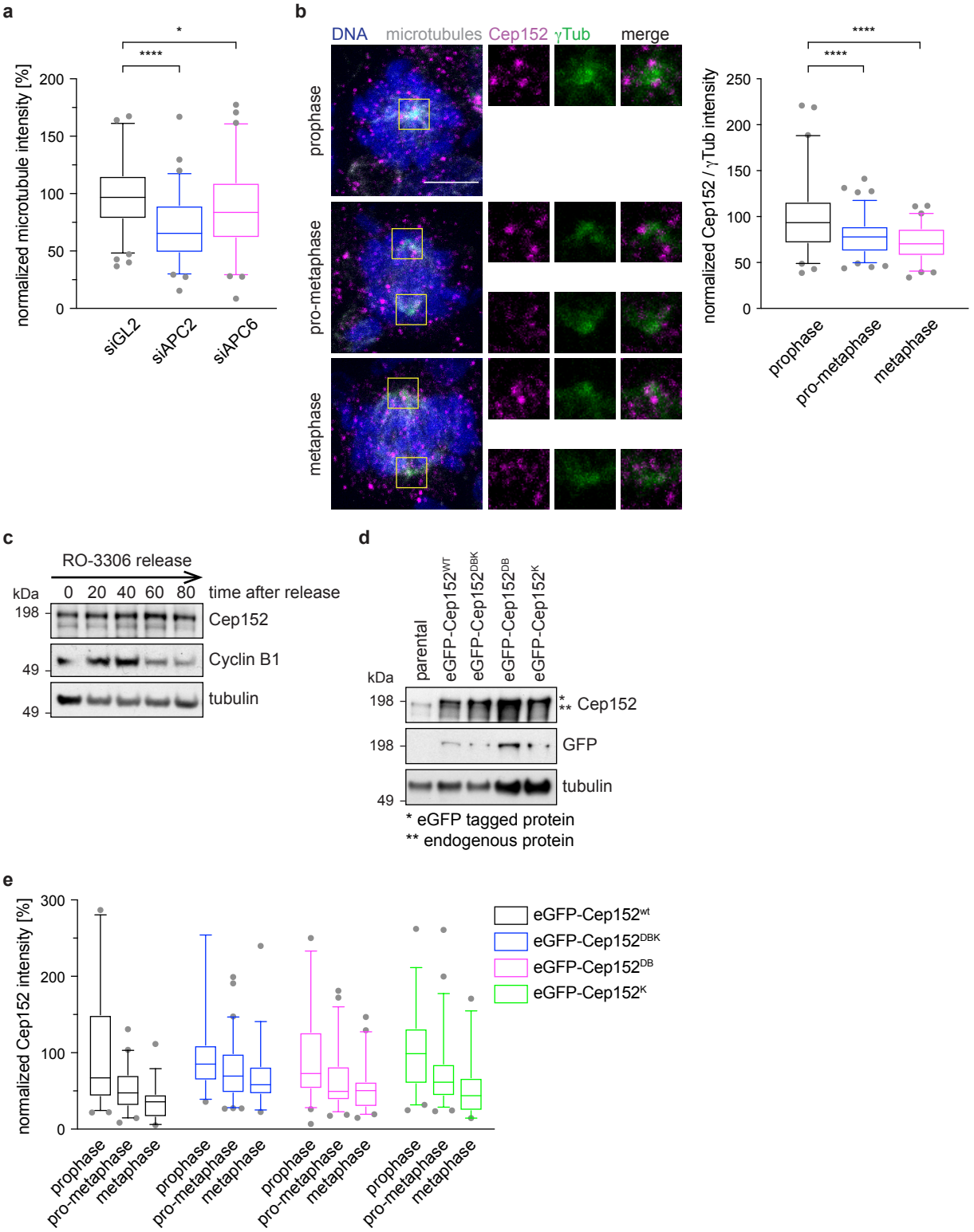

Cep152 protein levels at the centrosome decrease during mitosis. a, HEK293 cells shown in **Figure 5b** were stained against tubulin and its fluorescence intensity was measured and normalized against the GL2 control. N = 60 (siGL2), 60 (siAPC2), 62 (siAPC6). *P = 0.05, ****P < 0.0001 using a simple one-way ANOVA test with Dunnett's multiple comparison. **b**, Cells were treated according to the time line in **Figure 1e** and stained against the indicated proteins. The fluorescence intensity of Cep152 at the centrosome was measured and normalized against the intensity in prophase. Scale bars are 5 µm in the overview and 1 µm in the inset. N = 72 (prophase), 92 (pro-metaphase), 68 (metaphase). ****P < 0.0001 using a simple one-way ANOVA test with Dunnett's multiple comparison. **c**, Cells were treated according to the time line in **Figure 1e** and whole cell lysates were prepared at the indicated time points. The lysates were probed by immunoblot against the indicated proteins. **d**, HEK293 Flp-In T-Rex cells carrying the indicated eGFP-Cep152 variants were treated with tetracycline to induce the expression of the transgenes. Whole cell lysates were prepared and probed by immunoblot against the indicated proteins. Note that eGFP-Cep152 runs minimally higher as the endogenous protein. **e**, Complete dataset of the data shown in **Figure 5d**. The eGFP-Cep152WT and eGFP-Cep152DBK data are shown again for comparison. HEK293 FlpIn T-Rex cell lines expressing eGFP-Cep152 mutant proteins were treated as shown in **Figure 1e** and stained. The fluorescence intensity of eGFP-Cep152 at the centrosome was measured and normalized against the intensity of prophase cells of the corresponding cell line. N = 49 (DB, prophase), 39 (K, prophase), 55 (DB, pro-metaphase), 51 (K, pro-metaphase), 45 (DB, metaphase), 32 (K, metaphase).

Extended Data Figure 6

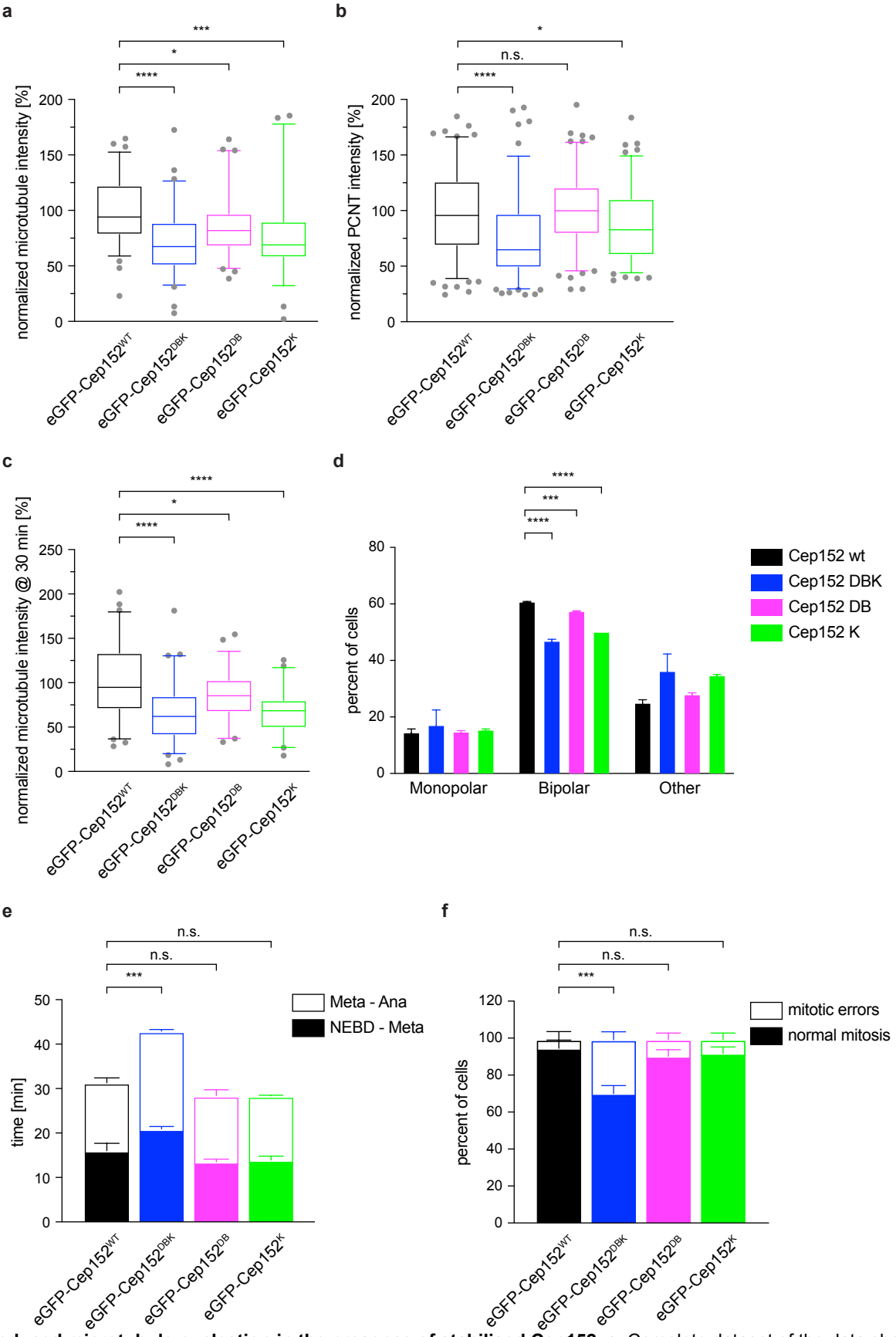

Reduced microtubule nucleation in the presence of stabilised Cep152. a, Complete dataset of the data shown in **Figure 6a**. The eGFP-Cep152WT and eGFP-Cep152DBK data are shown again for comparison. HEK293 FlpIn T-Rex cell lines expressing eGFP-Cep152 mutant proteins were treated as shown in **Figure 1e** and stained. The fluorescence intensity of tubulin was measured in the whole cell and normalized against the eGFP-Cep152WT cell line (right). N = 63 (DB), 57 (K). *P < 0.05, *** P < 0.001, ****P < 0.0001 using a simple one-way ANOVA test with Dunnett's multiple comparison. **b**, The fluorescence intensity of PCNT at the centrosome in cells from **a** was measured and normalized against the eGFP-Cep152WT cell line. N = 124 (DB), 110 (K). n.s. = not significant, *P < 0.05, ****P < 0.0001 using a simple one-way ANOVA test with Dunnett's multiple comparison. **c**, Complete dataset of the data shown in **Figure 6d**. The eGFP-Cep152WT and eGFP-Cep152DBK data are shown again for comparison. HEK293 FlpIn T-Rex cell lines were subjected to 45 min at 4 °C. The fluorescent intensity of tubulin was measured in the whole cell at the 30 min after shifting cells back to 37 °C and normalized against the eGFP-Cep152WT cell line (right). N = 52 (DB), 58 (K). *P < 0.05, ****P < 0.0001 using a simple one-way ANOVA test with Dunnett's multiple comparison. **d**, Cells shown in **Figure 6d** were analyzed for their spindle morphology after cold treatment for 45 min at 4 °C and recovery at 37 °C for 30 minutes. **e**, Cells from **Figure 6e** were analyzed for the time they need to progress from NEBD to metaphase (NEBD – Meta) and from metaphase to anaphase onset (Meta – Ana). Bar graphs show the mean +/- SEM. ***P = 0.0006 using a simple one-way ANOVA test with Dunnett's multiple comparison. N = 4 experiments, DB = 153 cells, K = 142 cells. **f**, Cells from **e** were analyzed for misaligned chromosomes during metaphase and lagging chromosomes during anaphase, combined as mitotic errors. Bar graphs show the mean +/- SEM. ***P = 0.0005 using a Holm-Sidak t-test. N = 4 experiments.

Extended Data Figure 7

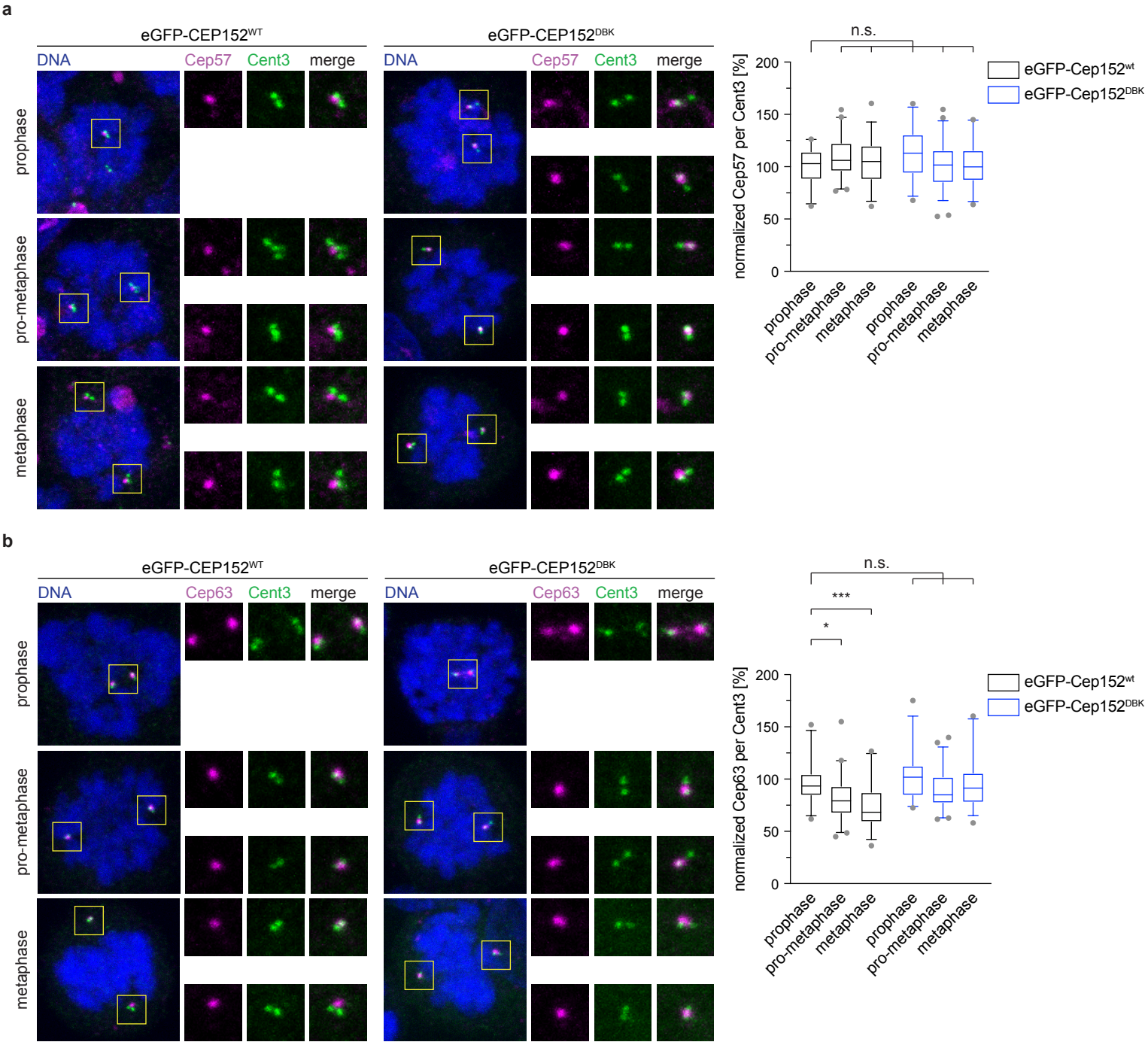

Localization of Cep57 and Cep63 during mitosis. a, **b**, HEK293 FlpIn T-Rex cell lines expressing eGFP-Cep152 Wt or DBK mutant protein were treated as shown in **Figure 1e** and stained with the indicated proteins (left). **a**, The fluorescence intensity of Cep57 was measured around the centrosome and normalized against prophase of the eGFP-Cep152WT cell line (right). N = 23 (prophase, WT), 48 (pro-metaphase, WT), 33 (metaphase, WT), 26 (prophase, DBK), 59 (pro-metaphase, DBK), 26 (metaphase, DBK). n.s. = not significant using a simple one-way ANOVA test with Dunnett's multiple comparison.. **b**, The fluorescence intensity of Cep63 was measured around the centrosome and normalized against prophase of the eGFP-Cep152WT cell line (right). N = 32 (prophase, WT), 56 (pro-metaphase, WT), 27 (metaphase, WT), 32 (prophase, DBK), 54 (pro-metaphase, DBK), 33 (metaphase, DBK). n.s. = not significant.*P < 0.05, *** P < 0.001, using a simple one-way ANOVA test with Dunnett's multiple comparison.